WILLIAMSON, EMILY ANN, M.S. Inhibition of Cytochrome P450 2E1, Cytochrome P450 3A6 and Cytochrome P450 2A6 by Citrus Essential Oils. (2010)
Directed by Dr. Gregory M. Raner, 66 pp.

Cytochrome P450 enzymes in the liver catalyze reactions involving the reduction of molecular oxygen and the oxidation of organic substrates. In some cases the resulting products may have the potential to contribute to oxidative stress within this organ. Oxidative stress usually involves the generation of very reactive compounds that can damage cellular components and are therefore harmful to the body. These reactive compounds can include hydrogen peroxide, superoxide, hydroxyl radicals, and a host of other metabolic intermediates (1). Oxidative stress occurs in alcoholics in the liver when an individual consumes harmful amounts of alcohol which can lead to the production of any one or more of the compounds listed above (2).

Cytochrome P450 enzymes have been linked to increased development of oxidative stress in the liver of alcoholics (2). Cytochrome $P450_{2E1}$ (CYP2E1) can cause mitochondrial stress and disruption via hydrogen peroxide productions which disturbs signaling pathways between cells (3). On the other hand, Cytochrome $P450_{2A6}$ (CYP2A6) has been shown to activate several known potent carcinogens found in tobacco smoke (4). Cytochrome $P450_{3A4}$ (CYP 3A4) is a widely recognized enzyme that plays a major role in the metabolism of pharmaceutical drugs, in fact more than 50% of all drugs are metabolized by this enzyme.

This study was designed to attempt to expand the knowledge of Cytochrome P450 inhibition by this series of citrus essential oils by studying their effects on Cytochrome $P450_{2E1}$, Cytochrome $P450_{3A4}$ and Cytochrome $P450_{2A6}$. Here the goal was to determine

if any of the nine citrus essential oils would inhibit any of the three Cytochrome P450 enzymes and if so then it would be determined how potent each citrus essential oil is and by what type of inhibition it occurred and determine the correlation between limonene, the main component in each citrus essential oil, and potency of each citrus essential oil. The results for CYP2E1 concluded that *Citrus tangerine*, tangerine, with a K_I value of 4 µg/mL was the most potent inhibitor and *Citrus aurantium*, neroli, with a K_I value of 14 µg/mL was the least potent inhibitor. The results for CYP3A4 concluded that none of the nine citrus essential oils inhibited the activity of CYP3A4 at a good quality concentration. Lastly, the results for CYP2A6 concluded that both *Citrus bergamia*, bergamot, and *Citrus aurantifolia*, lime, were the most potent inhibitors with a K_I of 0.81 µg/mL and a K_I of 1.4 µg/mL. It was concluded that bergamot oil contained 3.46 mM of limonene, grapefruit had 7.84 mM, lemon 4.24 mM, lime 3.75 mM, mandarin 3.79 mM, neroli 4.14 mM, orange 6.65 mM, and tangerine had 5.92 mM of limonene. Petitgrain oil was the only oil that a limonene concentration was unable to be detected, which is expected according to literature reviews which say petitgrain oil only has a 1-2 % content of limonene.

INHIBITION OF CYTOCHROME P450 2E1, CYTOCHROME P450 3A6 AND CYTOCHROME P450 2A6 BY CIRTUS ESSENTIAL OILS

by

Emily Ann Williamson

A Thesis Submitted to
The Facilty of The Graduate School at
The University of North Carolina at Greensboro
in Partial Fulfillment
of the Requirements for the Degree
Master of Science

Greensboro
2010

Approved by

_____
Committee Chair

To my Mother, Father, Family and Friends,
Without your love and encouragement this would not have been possible,
and to Michael,
Without your love and support none of this would have achievable,
Thank you all.

APPROVAL PAGE

This thesis has been approved by the following committee of the Faculty of The Graduate School at The University of North Carolina at Greensboro.

Committee Chair_____

Committee Members_____

_____

_____
Date of Acceptance by Committee

_____
Date of Final Oral Examination

ACKNOWLEDGEMENTS

First, I would like to thank Dr. Greg Raner for his guidance, support and encouragement throughout my undergraduate and graduate career at UNCG. I would also like to thank Dr. Nadja Cech for her support and guidance throughout my graduate career. Lastly, I would like to thank Dr. Alice Haddy for her support and guidance throughout my graduate career.

TABLE OF CONTENTS

Page

LIST OF TABLES vii

LIST OF FIGURES viii

CHAPTER

I. INTRODUCTION 1

I. A. Cytochrome P450 Enzymes 2
I. B. Cytochrome P450 2E1 7
I. B. i. CYP2E1 Active Site 8
I. B. ii. CYP 2E1 Role in Alcoholics 11
I. C. Cytochrome P450 3A4 12
I. C. i. CYP3A4 Active Site 13
I. C. ii. CYP 3A4 Role in Drug Metabolism 15
I. D. Cytochrome P450 2A6 15
I. D. i. CYP 2A6 Active Site 16
I. D. ii. CYP 2A6 Role in Tobacco Users 17
I. F. Citrus Essential Oils 18
I. F. i. Role in Humans 19

II. EXPERIMENTAL 21

II. A. Reagents: Source of all Purchased Chemicals 21
II. A. i. Preparation of Microsomes 21
II. B. CYP 2E1 Assays and Conditions 22
II. B. i. Initial Screening Assay for CYP 2E1 22
II. B. ii. HPLC Analysis 23
II. B. iii. Enzyme Kinetics Assay for CYP 2E1 and K_I Determination 23
II. C. CYP 3A6 Inhibition: Screening Essential Oils 24
II. C. i. CYP 3A6 Assays and Conditions 26
II. C. i. a. Inhibition Screening Assay for CYP 3A6 26
II. C. ii. HPLC Method Development and Analysis 27
II. D. CYP 2A6 Assays and Conditions 28
II. D. i. Initial Screening Assay for CYP 2A6 28
II. D. ii. HPLC Analysis 29

Page

II. D. iii. Enzyme Kinetics Assay for CYP 2A6 and K_I Determination 30
III. E. Limonene Analysis 31

III. RESULTS AND DISCUSSION 33

III. A. Inhibition of CYP 2E1 by Citrus Essential Oils 33
III. A. i. Enzyme Kinetics Analysis 36
III. B. Inhibition of CYP 3A6 by Citrus Essential Oils 40
III. C. Inhibition of CYP 2A6 by Citrus Essential Oils 48
III. C. i Enzyme Kinetics Analysis for CYP 2A6 56
III. D. Limonene Analysis 59

IV. CONCLUSION 63

REFERENCES 65

LIST OF TABLES

Page

Table I. 1: Literature results of the total content of limonene found in citrus essential oils grapefruit, orange, tangerine, mandarin, lemon, lime, bergamot, neroli, and petitgrain 18

Table III. 1: Averaged K_I values and error values calculated for CYP 2E1 inhibition activity by the nine citrus essential oils examined 37

Table III. 2: K_I values calculated for CYP 2A6 inhibition activity by bergamot and lime citrus essential oils 56

Table III. 3: Average peak area values for the limonene content in each limonene standard dilution and in each of the oils examined, percent error for each experiment, and total calculated limonene concentration for each sample in mM and percent 62

LISTS OF FIGURES

Page

Figure I. 1: Cytochrome P450 prosthetic heme iron III center showing the covalent bond between the iron III center and the sulfur of the cysteine ligand 3

Figure I. 2: Spin states of the iron III center 4

Figure I. 3: Cytochrome P450 catalytic cycle showing the various oxidative states of the iron heme center and the spin states of the iron heme center 6

Figure I. 4: The two different pathways that can occur in the CYP450 catalytic cycle 6

Figure I. 5: CYP 2E1 catalyzed reaction of the oxidation of p-nitrophenol to nitrocatechol 8

Figure I. 6: Stereo views of CYP 2E1 active site showing the ligand containing active site, small distal void, and access channel 10

Figure I. 7: Structure of CYP 2E1 with p-nitrophenol bound in the active site showing the amino acid residues involved in the reaction 11

Figure I. 8: CYP 3A4 catalyzed reaction of the oxidation of nifedipine to oxidized nifedipine 13

Figure I. 9: Secondary structures of the active site of CYP 3A4 showing the different helices, β-sheets, loops and channels 14

Figure I. 10: CYP 2A6 catalyzed reaction of the hydroxylation of coumarin to 7-hydroxycoumarin 16

Figure III. 1: Graph of percent activity of CYP 2E1 using human liver microsomes in the presence of 50 μM p-nitrophenol and different essential oils from 0.0 μg/mL to 3.8 μg/mL 34

Figure III. 2: Graph of percent activity of CYP 2E1 using human liver microsomes in the presence of 50 μM p-nitrophenol and different essential oils from 0.0 μg/mL to 3.8 μg/mL 36

Figure III. 3: Plot of area vs. p-nitrophenol (μM) concentration in the presence (pluses) and absence (triangles) of tangerine oil 39

Page

Figure III. 4: Plot of area vs. p-nitrophenol (µM) concentration in the presence (pluses) and absence (triangles) of neroli oil.....40

Figure III. 5: Graph of the amount of oxidized nifedipine produced by rabbit liver microsomes, a source of CYP 3A6, with increasing amounts of microsomes from 0.02 µg/mL to 0.08 µg/mL, 10 µM nifedipine, and a NADPH-regenerating system 42

Figure III. 6: Oxidized nifedipine and nifedipine standards HPLC chromatograms containing either oxidized nifedipine or 10 µM nifedipine and DI water and 2 % perchloric acid, but lacked NADPH.....44

Figure III. 7: Graph of percent activity of CYP 3A6 using rabbit liver microsomes in the presence of 10 µM nifedipine and different essential oils from 0.0 µg/mL to 3.0 µg/mL 46

Figure III. 8: Graph of percent activity of CYP 3A6 using rabbit liver microsomes in the presence of 10 µM nifedipine and different essential oils from 0.0 µg/mL to 3.0 µg/mL 48

Figure III. 9: 7-Hydroxycoumarin and coumarin standards HPLC chromatograms containing either 1.0 mM 7-hydroxycoumarin or 1.0 mM nifedipine and DI water and 6 % perchloric acid, but lacked NADPH.....49

Figure III. 10: Chromatogram of the screening data used for the initial screening inhibition experiment of lime oil on CYP 2A6 activity 52

Figure III. 11: Chromatogram of the screening data used for the initial screening inhibition experiment of bergamot oil on CYP 2A6 activity 53

Figure III. 12: Graph of percent activity of CYP 2A6 using rabbit liver microsomes, source of CYP 2A6, in the presence of 80 µM coumarin and different essential oils from 0.0 µg/mL to 3.0 µg/mL 54

Figure III. 13: Graph of percent activity of CYP 2A6 using rabbit liver microsomes, source of CYP 2A6, in the presence of 80µM coumarin and different essential oils from 0.0 µg/mL to 3.0 µg/mL 55

Figure III. 14: Plot of area vs. coumarin concentration, best representative, in the presence (pluses) and absence (triangles) of lime oil (0.50 µM) 58

Page

Figure III. 15: Plot of area vs. coumarin concentration, best representative, in the presence (pluses) and absence (triangles) of bergamot oil (0.50 µM). 59

Figure III. 16: Limonene standard curve showing the average peak area of limonene content in each standard dilution vs. total calculated limonene content. 61

CHAPTER I

INTRODUCTION

Cytochrome P450 enzymes catalyze reactions involving the reduction of molecular oxygen and the oxidation of organic substrates. These reactions can result in the production of compounds that may have the potential to contribute to oxidative stress within the liver or whatever tissue is exposed. Oxidative stress involves the generation of reactive compounds that can damage cellular components. These reactive compounds can include hydrogen peroxide, superoxide, hydroxyl radicals, and a host of other metabolic intermediates (1). Ethanol has been implicated in the induction of oxidative stress by increasing the amount of Cytochrome $P450_{2E1}$ (CYP 2E1) in the liver (5) and it has been shown that CYP 2E1 can cause mitochondrial stress and disruption via hydrogen peroxide production which disturbs signaling pathways between cells (3). Cytochrome $P450_{2A6}$ (CYP 2A6) has been shown to activate several known potent carcinogens found in tobacco smoke (4) and Cytochrome $P450_{3A4}$ (CYP 3A4) is a widely recognized enzyme that plays a major role in the metabolism of more than 50% of all pharmaceutical drugs on the market (6).

The purpose of this study was to attempt to expand the knowledge of Cytochrome P450 inhibition by a series of citrus essential oils by studying their effects on CYP 2E1, CYP 3A4 and CYP 2A6. The goal was to determine if any of the nine citrus essential oils would inhibit any of the three CYP450 enzymes and if so then it would be

determined how potent each citrus essential oil was and what type of inhibition occurred.An additional goal was to establish a link between the inhibition and certain known constituents of the oils such as limonene, which is the main component in each citrus essential oil, and potency of each citrus essential oil. The significance of this research is that if the oils inhibited the CYP450 activity it could prevent the production of reactive oxygen species (ROS) within the liver, where the enzymes reside. Each enzyme had a specific substrate that was used to monitor activity and to detect the amount of inhibition that was caused by each of the oils. Inhibition was analyzed using High Performance Liquid Chromatography (HPLC) and several methods were developed for more effective analysis. The amount of limonene in each oil was determined to establish if there the correlation between its content and the potency of the inhibitor. This was determined by using Gas Chromatography-Mass Spectrometry (GCMS).

I. A. Cytochrome P450 Enzymes

Cytochrome P450 enzymes (CYP450) are the most common Phase I enzymes. Phase I enzymes are drug metabolizing enzymes that are responsible for the metabolism, elimination, and/or detoxification of xenobiotics that enter the body through ingestion of food, beverages, drugs, natural products, cosmetics, and/or tobacco products (7). These enzymes are part of a very large family of hemeproteins that are made up of different families and subfamilies and are found in different spices including mammals, plants, and bacteria (8). **Figure I. 1** illustrates the heme iron III center that takes part in catalysis. As seen in this figure, the iron III center is bound to the nitrogens in the four surrounding

pyrrole rings and covalently bound to the sulfur in the cysteine ligand. Not shown in this figure is the sixth ligand that is bound to the iron III center which is a water molecule.

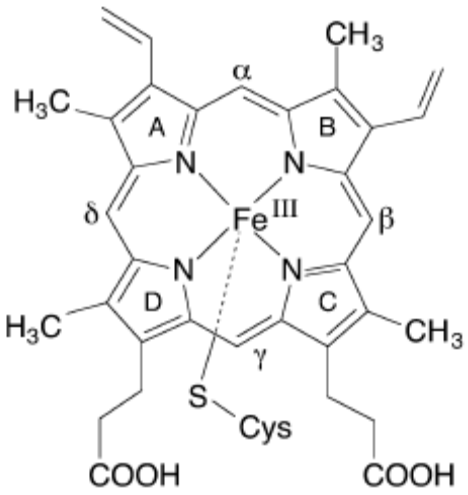

Figure I. 1: Cytochrome P450 prosthetic heme iron III center showing the covalent bond between the iron III center and the sulfur of the cysteine ligand. Also shown are side chains, four pyrrole rings labeled A-D, and the four nitrogen ligands surrounding the iron III center (8).

They are classified based on their similarities of their amino acid sequences identities and are located throughout the human body in the lungs, gastrointestinal tract, and kidneys, however they are most abundantly found in the liver (7). Many CYP450 enzymes catalyze a monooxygenase reaction in which the substrate (RH) gets one oxygen from molecular oxygen (O_2) incorporated into it (ROH) and the other oxygen forms a water

molecule (H_2O) with the input of two protons ($2H^+$) and two electrons (2e) as shown in **Equation I. 1** (8)**.**

$$RH + O_2 + 2H^+ + 2e^- \rightarrow ROH + H_2O \qquad \textbf{Equation I. 1}$$

The CYP450 catalytic cycle involves the reaction of the iron III center with a substrate, two electrons, two protons, and molecular oxygen. It begins the CYP450 in its resting state with the iron III (ferric iron) center in a low-spin state with all six of its ligands bound. When the substrate binds to the enzyme the water molecule is removed and the ferric iron center spin-state is changed to high-spin (9). This step is a result of the d orbital splitting where the low-spin state has one unpaired electron and change of symmetry to the ferric iron center when the water molecule is displaced changes the spin state to a high-spin state with 3 unpaired electrons (**Figure I. 2**).

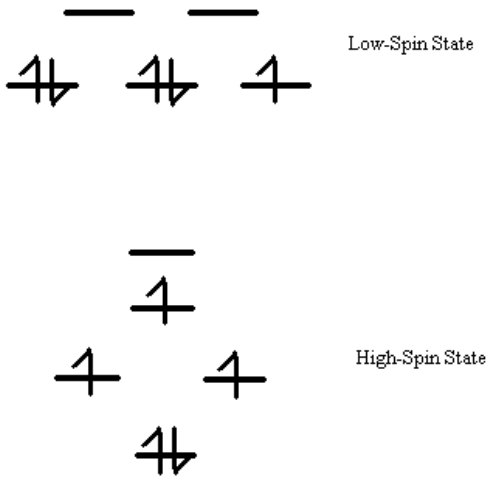

Figure I. 2: Spin states of the iron III center. Top: Low-spin state of the resting state of CYP450. Bottom: High-spin state after the water molecule has been displaced and the substrate is bound.

Figure I. 3 demonstrates the Catalytic cycle of CYP450. The first step (substrate binding) triggers the conversion of the low spin (LS) ferric iron III center of CYP450 to a high spin (HS) iron III center. Once the substrate is bound the redox potential is lowered and the ferric iron center can now be readily reduced to a ferrous iron II state via electron transfer from a reduced flavoprotein (CYP450 reductase) which accepts electrons from NADPH (step 2). In the ferrous iron state the iron II center binds to molecular oxygen due to its high affinity to bind and the same high-spin states of molecular oxygen and the iron II center (step 3). This step changes the spin-state back to low-spin where the ferrous iron bound to the oxygen is stabilized by resonance with an electron-transfer from the ferrous iron to the oxygen complex creating a ferric-superoxide (step 4). A second electron is transferred from the flavoprotein generating a ferrous superoxide complex (step 5), which is in resonance with the ferric peroxo complex (step 6). To finish the CYP450 catalytic cycle the now ferric-peroxo-complex is converted to a highly reactive oxoferryl intermediate with the addition of the two protons (step 7) (1), and in the presence of substrate, this species catalyzes the transfer of oxygen to the substrate regenerating the resting ferric state.

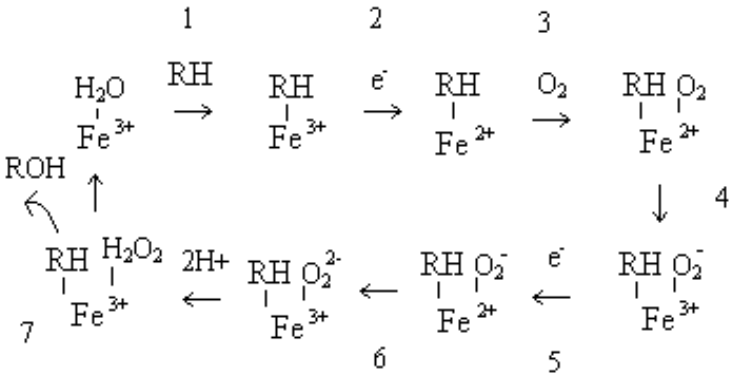

Figure I. 3: Cytochrome P450 catalytic cycle showing the various oxidative states of the iron heme center and the spin states of the iron heme center.

In the absence of substrate, a non productive release of H_2O_2 can also occur as shown in (**Figure I. 4**).

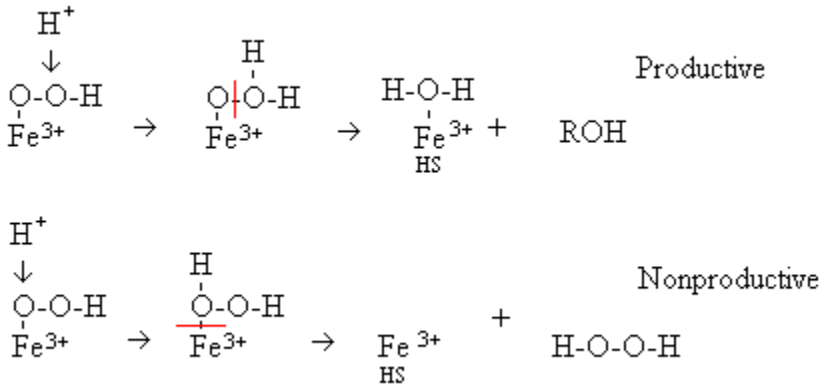

Figure I. 4: The two different pathways that can occur in the CYP450 catalytic cycle. Top: Productive pathway in which water is bound to the ferric iron center and the oxygenated substrate is formed. Bottom: Nonproductive pathway in which hydrogen peroxide is formed and dissociates from the ferric iron center.

The nonproductive pathway is a side reaction that occurs when uncoupling takes place within the cycle releasing the ferric iron center in high-spin and hydrogen peroxide, ROS. It can also occur when the substrate binding, oxygen binding, and electron delivery are not coordinated during the catalytic cycle (10). Hydrogen peroxide can then decompose into two hydroxyl radicals (**Equation I. 2**) which also causes oxidative stress.

$$H\text{-}O\text{-}O\text{-}H \rightarrow 2HO\bullet \qquad \textbf{Equation I. 2}$$

I. B. Cytochrome P450 2E1

Cytochrome P450 2E1 (CYP 2E1) is located in the liver but can also be found in the brain, lungs, and a variety of other tissues, thus CYP 2E1-induced oxidative stress can be a global problem in the human body. CYP 2E1 has been studied for its ability to metabolize ethanol, activate procarinogens, and its relationship to alcoholism, diabetes, and other diseases (10). In addition to H_2O_2 production, CYP 2E1 can generate toxic and carcinogenic compounds via activation of a number of pro-carcinogens (10). It has been shown that the levels of CYP 2E1 are highly elevated in the liver of alcoholics (11), which may contribute to the pathology of alcoholic liver disease. CYP 2E1 only plays about a 4% role in the metabolism of drugs, however its ability to metabolize carcinogens, organic solvents, industrial chemicals, and other toxins such as ethanol, benzene, lauric acid, acetone, and more make it a particularly good target for toxicological study (12).

CYP 2E1 is known to metabolize para-nitrophenol (p-NP) into nitrocatechol with a high binding affinity. The substrate p-nitrophenol is therefore a convenient probe for CYP 2E1 activity and was used to detect CYP 2E1 activity in this study. **Figure I. 5**

shows the reaction catalyzed by CYP 2E1 which oxidizes p-nitrophenol forming nitrocatechol.

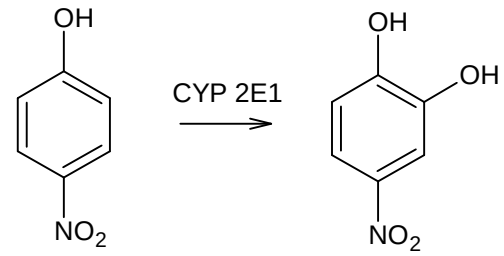

Figure I. 5: CYP 2E1 catalyzed reaction of the oxidation of p-nitrophenol to nitrocatechol.

I. B. i. CYP 2E1 Active Site

The active site of CYP 2E1 is relatively hydrophobic and small compared to most CYP450s. It is so small that it is one of the smallest active sites that has been discovered for CYP450 enzymes. P. R. Porubsky and colleagues have shown that the CYP 2E1 active site has two adjacent voids, one which is enclosed above the I helix and the other forms a channel to the protein surface. The volume of the active site is around 190 Å which explains why substrates for CYP 2E1 have low molecular weights. The amino acids that line the active site on the successive turn of the I helix are Ala299 and Thr303. The opposite side of the active site consists of an intersection of residues in and near the B' helix, which includes Phe106, Ile115, and Phe116, the loop between helix K and β_{1-4}, which includes Val364 and Leu368, and the β_{4-1}, / $\beta 4_{-2}$, turn, Phe478. There are five phenylalanine residues, Phe106, Phe116, Phe207, Phe298, and Phe478, which line the

roof of the active site (Patrick R. Porubsky, 2008). There is also an enclosed cavity that is located adjacent to the active site that has a volume of 77 Å and is formed by the amino acids His109, Leu202, Phe203, Asn206, Val239, Val242, Lys243, Ala294, and Asp295 (10). CYP 2E1 also has an access channel orientated adjacent to the active site opposite of the I helix and extending to the surface. It contains several water molecules and is separated from the active site by Phe478. Rotation of Phe478 residue would allow compounds to have direct communication with the active site. **Figure I. 6** shows four different views of the active site (10).

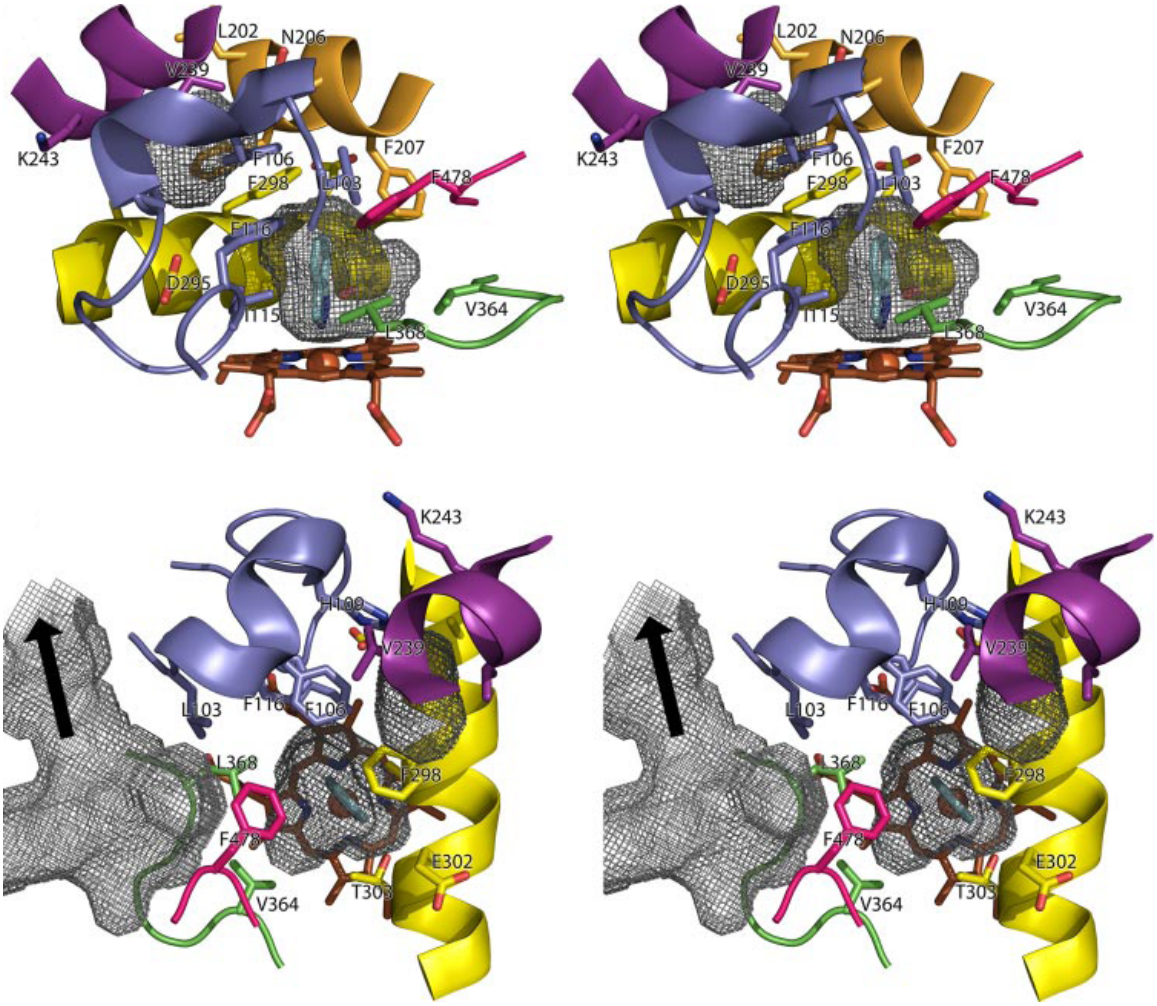

Figure I. 6: Stereo views CYP 2E1 active site showing the ligand containing active site, small distal void, and access channel. Figure displays cavities, B' helix and adjacent loop, F helix, G helix, I helix, loop between K and $\beta_{1\text{-}4}$, and β4-1/β4-2 turn. Top: access channel is omitted. Bottom: F helix is omitted (10).

The compounds that enter the active site of CYP 2E1 are restricted by the size of the active site, thus only low molecular weight compounds are able to enter the active site. The nonpolar phenylalanine residues that line the roof of the active site interact with aromatic compounds which explains why p-NP, an aromatic low molecular weight

compound, is a favorable substrate for CYP 2E1. **Figure I. 7** shows the orientation of p-NP in the active site of CYP 2E1 (11). The residues that interact with p-NP are Phe478, Leu368, Thr303, and Ala299 as well as the heme iron center. Residues Val364, Pro365, Ser366, Asp367 and Leu368 have stabilizing interactions with p-NP (11).

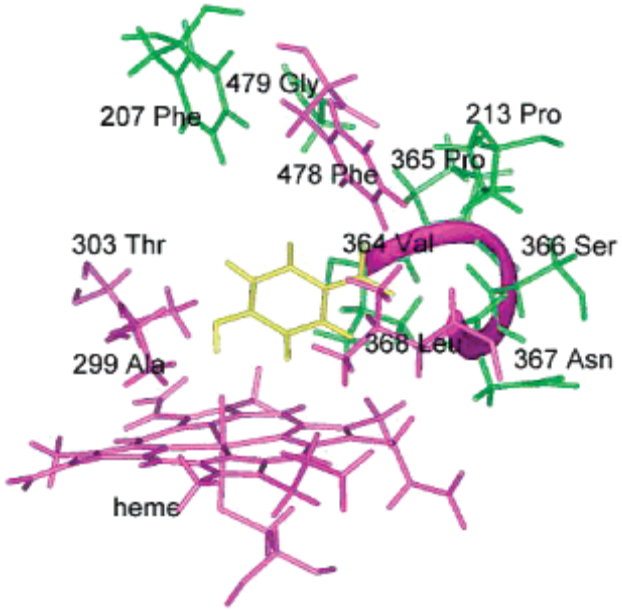

Figure I. 7: Structure of CYP 2E1 with p-nitrophenol bound in the active site showing the amino acid residues involved in the reaction (11).

I. B. ii. CYP 2E1 Role in Alcoholics

Ethanol-induced oxidative stress has been shown to play a major role in the mechanism by which ethanol causes liver damage. The CYP 2E1 pathway contributes to the ability of ethanol to induce oxidative stress by metabolizing and activating ethanol to

a more reactive and toxic product acetaldehyde. It has been shown that a decrease in CYP 2E1 induction was associated with a reduction in alcohol-induced liver damage (5). Diallyl sulfide, phenethyl isothiocyanate, and chlormethiazole have been shown to inhibit CYP 2E1 (5). Autoantibodies against CYP 2E1 have been discovered in the liver of alcoholics that recognize hydroxyl radicals (13), further illustrating the significance of this mechanism for oxidative damage resulting from the CYP 2E1 enzyme. These observations suggest that CYP 2E1 inhibitors may represent a viable therapeutic tool to prevent oxidative stress.

I. C. Cytochrome P450 3A4

Cytochrome P450 3A4 (CYP 3A4) is located mainly in the liver but can also be found in the small intestines, lungs, stomach, and colon. Other CYP 3A subfamily enzymes can be produced in the kidneys, prostate, testis and thymus however the 3A4 isoform is not. It is the most abundant CYP450 enzyme in the human body metabolizing around 30% of all drugs which is more than any other CYP450 enzyme (13). It has been discovered that in fetal livers the most abundant enzyme is CYP 3A7 and CYP 3A4 is expressed at low levels. After birth the expression of CYP 3A4 increases rapidly and reaches 50% of adults level expression at the age of 6 to 12 months after birth (13). CYP 3A4 has been shown to have at least three binding sites (14).

CYP 3A4 is known to metabolize nifedipine into oxidized nifedipine, thus the substrate nifedipine is a useful marker used to probe CYP 3A4 activity. This substrate was therefore used in the current study to monitor inhibition. It should be noted also, that the rabbit produces a related isoform CYP 3A6 that can be used as a model for the human

CYP 3A4 enzyme, with very similar catalytic activities. The current study utilizes rabbit tissue rather than human tissue. **Figure I. 8** shows the reaction catalyzed by CYP 3A4 which oxidizes nifedipine forming oxidized nifedipine.

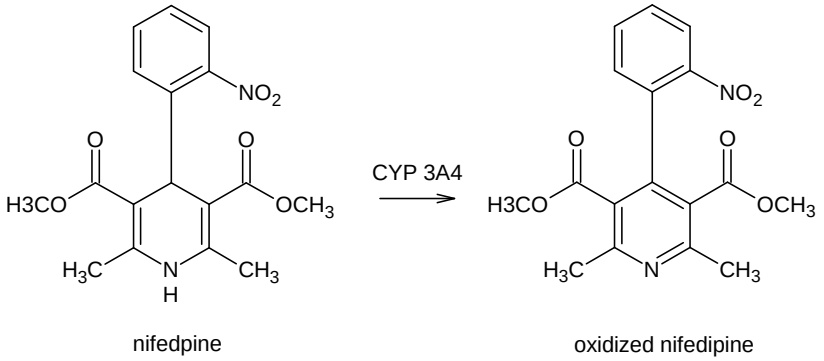

nifedpine oxidized nifedipine

Figure I. 8: CYP 3A4 catalyzed reaction of the oxidation of nifedipine to oxidized nifedipine.

I. C. i. CYP3A4 Active Site

The active site of CYP 3A4 is very large and hydrophobic. The size of the active site is why CYP 3A4 is able to metabolize a broad range of compounds with very high molecular weights. Due to the lipophlic character of the active site hydrophobic interactions are largely responsible for substrate binding (15). The volume of the active site is around 600 Å in size. The active site of CYP 3A4 is made up of many different amino acids but the amino acids that form the catalytic center of CYP 3A4 and have a role in substrate binding are Leu210, Leu211, and Asp214. These amino acids residues are located in the F-helix which is isolated from the iron heme center (15). **Figure I. 9** shows two different views of the active site of CYP 3A4. The active site of CYP 3A4

consist of five substrate channels, 2a, 2b, 2c, 2e, and 3 and one solvent channel, S. These channels are defined depending on the secondary structure that exhibits the entrance and exit of the channel. Channel 2a is located in the active site of CYP 3A4 between the FF' loop and the β1 sheet and β4 sheet and has a length of 19 Å. Channel 2b has a length of 18 Å and is situated between the F' helix, G' helix and the β1 sheet and the BC loop. The 2c channel has a length of 17 Å and is positioned between the GG' helix and the BC loop and channel 2e is beside the BC loop as well with a length of 12 Å. Channel 3 passes through the F' helix as well as the G' helix with a length of 17 Å and the S channel is located above the I helix and between the FF' loop and the β4 sheet with a length of 13 Å (16).

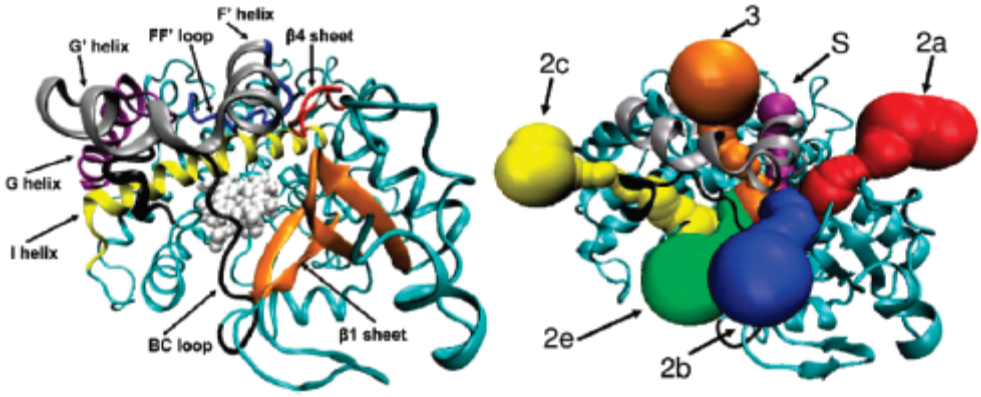

Figure I. 9: Secondary structures of the active site of CYP 3A4 showing the different helices, β-sheets, loops and channels. Left: FF' loop, F' helix, G' helix, G helix, I helix, BC loop, β1 sheet, and β4 sheet. The heme iron center is white. Right: Channel surfaces; channel 2a, channel 2b, channel 2c, channel 2e, channel 3, and channel S. F' and G' helices are shown as well as the BC loop. (16).

The orientation and the interactions for the substrate nifedipine and the active site of CYP 3A4 are highly specific. The nitro group on nifedipine forms a hydrogen bond with the amino acid residue Ser113. This hydrogen bond, together with other interactions with active site amino acid residues, help position nifedipine for the N-oxidation reaction it undergoes. The hydrogen that is attached to the nitrogen ring is oriented so that it lies directly above the heme iron center (17).

I. C. ii. CYP 3A4 Role in Drug Metabolism

CYP 3A4 enzymes pose a problem in drug development and clinical use of drugs because of its interactions with drug disposition and/or drug-drug interactions. CYP 3A4 metabolizes a high percentage of drugs that enter the human body. A high level of enzyme activity toward a drug causes a decrease in that drugs bioavailability (13) conversely, drugs, or compounds, that inhibit this isoform can reduce the normal metabolism of another drug, causing elevated levels and potential toxic side effects. It has been reported that the interaction between CYP 3A4 and herbal medicines is one of the worst problems that CYP 3A4 enzymes cause. Saint John's Wort interactions with CYP 3A4 has been one of the most studied relationships. Saint John's Wort increases the activity of CYP 3A4 which in turn decreases the effectiveness of oral contraceptives (18).

I. D. Cytochrome P450 2A6

Cytochrome P450 2A6 (CYP 2A6) is mainly found in the liver but can also be found in other tissues including trachea, lung, nasal mucosa, and esophageal mucosa. However, it is expressed at medium to low levels in the human liver. CYP 2A6 metabolizes less than 5% of all drugs and is studied for its effect in liver cancers (13).

CYP 2A6 is also responsible for the detoxification of nicotine in the human body and for the activation of tobacco specific carcinogens (19).

CYP 2A6 is the only CYP 450 enzyme known to catalyzes the 7-hydrooxylation of coumarin. Coumarin is therefore the ideal compound to probe for the activity of CYP 2A6 (13). **Figure I. 10** shows the reaction catalyzed by CYP 2A6 which is the 7-hydroxlyation of coumarin.

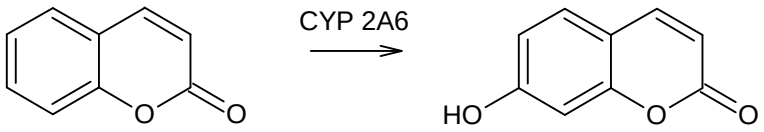

coumarin 7-hydroxycoumarin

Figure I. 10: CYP 2A6 catalyzed reaction of the hydroxylation of coumarin to 7-hydroxycoumarin.

I. D. i. CYP 2A6 Active Site

The active site of CYP 2A6 is small, compact, and hydrophobic (20). It is the most abundant of the three members of the CYP 2A subfamily (21). CYP 2A6s active site has only one amino acid that is able to be a hydrogen bond donor, Asn297. Asn297 is the amino acid that orientates the coumarin substrate so that it is able to be oxidized properly (20). Asn297 is orientated in the proper direction with help from its neighboring amino acids (20). Another important interaction between the amino acids in the active site and the substrate is the interaction between Phe107 and aromatic or planar substrates, which help s to explain selectivity of this enzyme. Other amino acids that line the active

site of CYP 2A6 include Tyr114, Gly115, Phe118, Val117, and Met293. The compounds that enter the active site of CYP 2A6 are compounds that are small planer and adapted for oxidation (19). Coumarin is the ideal substrate for CYP 2A6 and has been shown to only be metabolized by CYP 2A6 (13). The active site of CYP 2A6 binds with coumarin in a specific way with a hydrogen bond between Asn297 and coumarin which orientates coumarin for the 7-hydroxylation reaction that it undergoes.

I. D. ii. CYP 2A6 Role in Tobacco Users

Tobacco use has been associated with cancers for a long time. Including cancers of the lung, larynx, mouth, esophagus, kidneys, and urinary tract. The CYP450 enzymes are able to metabolize tobacco carcinogens into DNA-binding metabolites (22), in particular, nitrosamines. CYP 2A6 enzymes also play a role in catalyzing the metabolism of many environmental chemicals including coumarin, nicotine, and several tobacco-specific carcinogens (23). For example, CYP 2A6 are the main catalyst involved in the metabolism of nicotine to cotinine via 3'-hydroxylation (13). The inhibition of CYP 2A6 has recently been identified as a possible therapeutic approach to smoking cessation, thus giving significance to the current study, whose goal is to identify natural products with the ability to inhibit this isoform. Of significance also is the fact that inhibition of CYP 2A6 may reduce the ability of this enzyme to activate pro-carcinogens into carcinogenic products. For example CYP 2A6 also catalyzes the 2'-hydroxylation of nicotine which is a known precursor of lung carcinogens (13). It has been shown that individuals who lack the CYP 2A6 enzyme have impaired nicotine metabolism and may

be protected against tobacco dependence (22), and possibly some of the carcinogenic effects of these products.

I. F. Citrus Essential Oils

The most commonly known fact about essential oils is that they are used during massages, for aromatherapy and used as food additives. An essential oil is the volatile lipid-soluble portion of the fluids of a plant that contains odiferous compounds (24). Such fluids are produced through steam distillation of the plant matter which can be any part of the plant including the stem, branch, fruit, flower, leaf, seed, root, bark, etc. Essential oils are made up of hundreds of compounds and are very complex substances. One thing that citrus essential oils have in common is that they all have the compound limonene present in them. **Table I. 1** shows the literature research results of the amount of limonene found in different citrus essential oils.

Oil	% Limonene
Limonene	95%
Grapefruit	86-92 %
Orange	85-90 %
Tangerine	65-80 %
Mandarin	65-75 %
Lemon	55-75 %
Lime	34-64 %
Bergamot	25-40 %
Neroli	9-18 %
Petitgrain	1-2 %

Table I. 1: Literature results of the total content of limonene found in citrus essential oils grapefruit, orange, tangerine, mandarin, lemon, lime, bergamot, neroli, and petitgrain.

I. F. i. Role in Humans

There are four common ways to ingest essential oils, through inhalation by the lungs, absorbance through the skin, through the digestive tract from oral administration, and from absorbance of our bodies' orifices (24). There are different opinions of the best ways to administer essential oils. According to David Stewart, who wrote "The Chemistry of Essential Oils: Made Simple", Germans think inhalation through the lungs is the most effective way to obtain the benefits of essential oils, the English think absorbance through the skin from messages is the most effective, and the French think that taking them orally is the most effective. Over 95% of essential oils are produced for flavoring of foods and fragrances for perfumes. In humans essential oils can be used as a nutritional supplement such as borage oil, coconut, garlic, etc. An advantage that essential oils have is that the compounds that make them up are very small and can therefore easily enter by our bodies. The essential oils also act as competitive inhibitors which is when a reversible inhibitor binds to the active site of an enzyme taking the place of the substrate and competing with the substrate for binding (25). Mitsuo Miyazawa, et al have reported studies that show CYP450 enzymes are responsible for the metabolism of limonene in animals such as rats, mice, rabbits, guinea pigs, and even dogs. The CYP450 enzymes located in liver microsomes from these animals oxidize limonene to different oxidized products including 1,2-epoxides, 8,9-epoxides, a 6-hydroxylation which produces carveol, and a 7-hydroxylation which produces perillyl alcohol (26).

In the current study we have examined the ability of a variety of citrus essential oils to inhibit the activities of CYP 2E1, 3A6, and 2A6. Essential oils are natural products that are presumed to be safe for human consumption. Essential oils could be an important class of products for reducing oxidative stress because of the compounds found in them and what they are able to do. For example, compounds such as bergaptol and geranylcoumarin, found in grapefruits, act as radical scavengers (27). Essential oil components such as linalol, linalyl acetate, and monoterpene esters have shown to have beneficial effects to human health by acting as an anti-inflammatory (28). Studies have also shown that essential oils have antibacterial effects. For example, when added to mouthwash essential oils cause cell lysis in the organisms that are responsible for plaque and gingivitis (29). Essential oils have strong activity against the Gram-positive microbes that cause plaque and gingivitis. There have also been reports that show that essential oils have mild antifungal effects however they are not as strong as antibiotics (30). Essential oils have the potential to reduce the production of H_2O_2, OH radicals and the activation of carcinogens by CYP 2E1 enzymes, reduce drug interactions by CYP 3A4 enzymes, and act as a possible therapeutic approach to smoking cessation and as an anti-cancer agent by inhibiting CYP 2A6 activity.

CHAPTER II

EXPERMIENTAL

II. A. Reagents: Source of all Purchased Chemicals

The chemicals that were used during these studies were purchased from different companies. The p-nitrophenol, nitrocatechol, nifedipine, coumarin, 7-hydroxycoumarin, and limonene were purchased from Sigma-Aldrich. Oxidized nifedipine was purchased from Oxford Biomedical. The human liver microsomes that were used in the CYP 2E1 assays was purchased from Moltox in Asheville, North Carolina and the rabbit livers were purchased from Pel-Freeze in Rogers, Arkansas. The citrus essential oils were purchased from Birch Hill Happenings Aromatherapy, LLC in Barnum, Minnesota.

II. A. i. Preparation of Microsomes

Rabbit liver microsomes were generated in the lab using whole rabbit livers. The rabbit livers were first homogenized in a 50 mM potassium phosphate buffer, pH 7.4, which contained 0.1 mM EDTA. Once homogenized, the mixture was centrifuged using a JA-10 centrifuge rotor at 4420 x g for 10 minutes at 4°C. The pellet in the mixture was discarded and the supernant was centrifuged using a JA-20 centrifuge rotor at 37000 x g for 60 minutes at 4°C. Lastly, the pellet was resuspended in a minimal volume of the homogenization buffer described above. Microsomes were then separated into 200 µL aliquots and stored at -80°C.

II. B. CYP 2E1 Assays and Conditions

Enzyme kinetics studies have been used to look at the effects of citrus essential oils on CYP2E1. The oils include *Citrus bergamia, Citrus paradisi, Citrus limon, Citrus aurantifolia, Citrus reticulata, Citrus aurantium, Citrus sinensis, Citrus aurantium,* and *Citrus nobilis.* These oils are also commonly known as bergamot, grapefruit, lemon, lime, mandarin, neroli, orange, petitgrain, and tangerine. Limonene was also evaluated for its effect on CYP 2E1.

II. B. i. Initial Screening Assay for CYP 2E1

The assay that was used to measure the amount of inhibition of CYP 2E1 involved the oxidation of p-nitrophenol to nitrocatechol. Each inhibitor was diluted by taking 5 µL of oil and dissolving it in 100 mL of water to make a stock solution. Conditions for the screening assay involved 25 µL of human liver microsomes (approximately 1 mg/mL total protein concentration) being incubated at 37°C for 30 minutes in a reaction mixture containing 100 mM potassium phosphate buffer (pH 7.4), 50 µM of p-NP, DI water, and various amounts of each oil (ranging from 0.1 µg/mL to 3.0 µg/mL), added to give a volume of 475 µL. Each sample was vortexed and placed into a hot water bath for one minute prior to the addition of NADPH. The reaction was initiated using 25 µL of NADPH to give a final total volume of 500 µL. Following the 30 minute incubation at 37°C the protein was precipitated out with 0.20 mL of 6 % perchloric acid and placed on ice for 10 minutes. Samples were centrifuged for 10 minutes at 3500 rpm and 460 µL of the clear supernant solution were placed in HPLC vials and analyzed by HPLC.

II. B. ii. HPLC Analysis

The reactions were then analyzed via HPLC. The HPLC analysis was conducted using Shimadzu's LC-20AT/ Prominence Liquid Chromatography system and the samples were detected by the SPC-20A/ Prominence UV/Vis Detector at 340 nm. Up to 100 vials were loaded into the Autosampler and a 40 µL sample of each sample was injected onto a 150 mm x 4.6 mm C_{18} HPLC column at a flow rate of 1.0 mL/min. The mobile phases used for this method consisted of two solutions, acetonitrile with 0.5 % acetic acid (A) and DI water with 0.5 % acetic acid (B). The mobile phases were set at 20 % A and 80 % B respectively. The product, nitrocatechol, had a retention time of 5.60 minutes under these conditions. The nitrocatechol peaks from each of the reaction samples were integrated to give peak areas, which reflected the relative activities of CYP 2E1 in human liver samples.

II. B. iii. Enzyme Kinetics Assay for CYP 2E1 and K_I Determination

Conditions used for the enzyme kinetics assay involved liver microsomes being incubated at 37°C for 30 minutes in a reaction mixture containing a range of p-NP from 20 µM to 160 µM, 100 mM potassium phosphate buffer (pH 7.4), a specified concentration of the inhibitor (between 0.0 and 3.75 mg/mL), and DI water to give a volume of 475 µL. Each sample was vortexed and placed in the hot water bath for one minute. The reaction was initiated with the addition of 25 µL of NADPH to give a final total volume of 500 µL. A control reaction was run with each experiment that was the same as above only the inhibitor was replaced with water. Following the 30 minute incubation at 37°C the reaction was quenched and the protein was precipitated out with

0.20 mL of 6 % perchloric acid and placed on ice for 10 minutes. Samples were centrifuged for 10 minutes at 3500 rpm and 460 µL of the clear supernant solution was placed in HPLC vials to be analyzed by HPLC.

The Michaelis Menten model of enzyme kinetics was used in order to determine the apparent K_I for each oil, expressed as mg oil / mL. Each K_I was found by plotting the relative activity (V) vs. substrate concentration ([S]) at a range of increasing concentration of p-NP in the presence or absence of inhibitor. The concentration of inhibitor, [I], was chosen based on the conditions of the screening experiments carried out for each oil where the conditions gave ~50 % inhibition of CYP 2E1. The Slide Write Plus (by Advanced Graphics Software, Inc.) program was used to plot the relative activity vs. concentration of p-NP. The Michaelis-Menten equation (**Equation II. 1**) was used to determine the V_{max}, $V_{max\ app}$, K_m, and $K_{m\ app}$.

$$V_o = \frac{V_{max} * [S]}{K_m + [S]} \qquad \textbf{Equation II. 1.}$$

The K_I was calculated using the inhibitor concentration and **Equation II. 2**.

$$K_{m\ app} = K_m (1 + [I]/K_I) \qquad \textbf{Equation II. 2.}$$

These equations were used because it characterizes a competitive model of inhibition and the $V_{max\ app}$ in each case was within 20 % of V_{max} demonstrating that a competitive mode of inhibition was the primary effect.

II. C. CYP 3A6 Inhibition: Screening Essential Oils

Initially, an assay was developed to determine the amount of oxidized nifedipine was produced in the reaction of rabbit liver microsomes with nifedipine. Microsomes were used as the source of CYP 3A4. Reaction conditions were optimized in order to

generate sufficient product for subsequent inhibition studies. It was first determined that the reactions were producing increasing amounts of oxidized nifedipine with increasing amounts of rabbit liver microsomes. To do this, an assay was developed which included increasing amounts of a rabbit liver microsomes (approximately 1 mg/mL total protein concentration), DI water, potassium phosphate buffer containing 3.3mM $MgCl_2$, (pH 7.4, 100 mM), and 10 μM nifedipine to give a volume of 412.5 μL. Each sample was vortexed and placed in a 37°C hot water bath for one minute prior to the addition of the NADPH-regenerating system, which would give a final total volume of 500 μL. The reaction was initiated with the addition the NADPH-regenerating mixture which consisted of a 100 mM potassium phosphate assay buffer containing 3.3mM $MgCl_2$, (pH 7.4), 33 mM glucose-6-phosphate, NADP+ (1mM), glucose-6-phosphate dehydrogenase (1 unit/mL), and DI water. The NADPH-regenerating system was incubated for 7 minutes at 37°C prior to it's' addition to each of the samples. Incubation continued for one hour at 37°C after the NADPH-regenerating system was added to each sample. Controls were run with each experiment that replaced NADPH with water. Following the one hour incubation each sample was quenched with 500 μL of CH_2Cl_2 and 500 μL each of 0.1M Na_2CO_3 and 0.2 M NaCl. Each sample was vortexed for 30 seconds and centrifuged for 10 minutes to separate the two layers. The lower organic level was removed and inserted into a centrifuged tube and centrifuged under a nitrogen steam until dry. The contents were dissolved in a 500 μL of 64% methanol/36%water solution and 500 μL samples were placed into HPLC vials and injected into the HPLC for analysis (6).

An alternative method was also developed in which reactions were quenched with acid and following centrifugation were injected directly onto the HPLC. To quench the reaction, two types of acid were examined 6% perchloric acid and 35% trichloro acetic acid. When using these acids as a quench 200 µL were used to quench the reaction. After the one hour incubation each sample was quenched with acid and placed in ice for 10 minutes then centrifuged at 3000 rpm for 15 minutes. Samples were then added to HPLC vials and loaded into the HPLC for analysis.

II. C. i. CYP 3A6 Assays and Conditions

Enzyme kinetics studies were used to study the effect of the following essential oils: *Citrus bergamia, Citrus paradisi, Citrus limon, Citrus aurantifolia, Citrus reticulata, Citrus aurantium, Citrus sinensis, Citrus aurantium,* and *Citrus nobilis* on CYP 3A4. In addition, the pure compound limonene was also evaluated for its effect on CYP 3A4 activity.

II. C. i. a. Inhibition Screening Assay for CYP 3A6

Each inhibitor was diluted by taking 5 µL of oil and dissolving it in 100 mL of DI water to make a stock solution. Conditions for the screening assay involved 25 µL of rabbit liver microsomes (approximately 1 mg/mL total protein concentration) being incubated at 37°C for 30 minutes in a reaction mixture containing DI water, 100 mM potassium phosphate buffer containing 3.3mM $MgCl_2$, (pH 7.4), various amounts of each oil (ranging from 0.1 µg/mL to 3.0 µg/mL), and 10 µM nifedipine to give a volume of 413 µL. Each sample was vortexed and placed in a 37°C hot water bath for one minute followed by the addition of 87 µL of the NADPH-regenerating system to give a final total

volume of 500 µL. The reaction was initiated with the addition the NADPH-regenerating system. The reaction continued for one hour at 37°C after the NADPH-regenerating system was added to each sample. Controls were run with each experiment that replaced NADPH with water. Following the one hour incubation at 37°C the protein was precipitated out with the addition of 0.20 mL of 6 % perchloric acid and the resulting solutions were placed on ice for 10 minutes. Samples were centrifuged for 15 minutes at 3000 rpm and 460 µL of the clear supernant solution was placed in HPLC vials to be analyzed by HPLC (6).

II. C. ii. HPLC Method Development and Analysis

To analyze the amount of nifedipine oxidized by CYP 3A4, several methods were examined using HPLC. The HPLC analysis was conducted using Shimadzu's LC-20AT/ Prominence Liquid Chromatography system and the samples were detected by the SPC-20A/ Prominence UV/Vis Detector at 254 nm. Up to 100 vials were loaded into the autosampler and a 40 µL aliquot of each sample was injected onto a 150mm x 3.2 mm 5 micron C_{18} column at a flow rate of 0.6 mL/min and a run time of 8 minutes. Different mobile phases were evaluated using a two solvent system consisting of 100% methanol (A) and 0.5% acetic acid in DI water (B). A 50/50 mixture of A and B was initially used, but peaks were not sharp or well resolved. The peaks were joined together, which prevented accurate integration of the peak areas. The mobile phases were then changed to a 60/40 solution of A and B giving baseline separation of the product, therefore facilitating its accurate quantification. Standards were used to differentiate between the nifedipine and oxidized nifedipine peaks. The nifedipine eluted off the column at 5.00

minutes and was determined by injecting a nifedipine standard solution consisting of nifedipine, DI water, and 6 % perchloric acid, into the HPLC. The product, oxidized nifedipine purchased from Oxford Biomedical, gave a retention time of 3.50 minutes under these conditions, as determined by injecting an authentic standard solution consisting of oxidized nifedipine, DI water, and 6 % perchloric acid, into the HPLC. The oxidized nifedipine peaks from each of the reaction samples were integrated to give the relative activities of CYP 3A4 in rabbit liver samples.

II. D. CYP 2A6 Assays and Conditions

Enzyme kinetics studies were used to study the effects of the following citrus essential oils, *Citrus bergamia, Citrus paradisi, Citrus limon, Citrus aurantifolia, Citrus reticulata, Citrus aurantium, Citrus sinensis, Citrus aurantium,* and *Citrus nobilis* on CYP 2A6. An authentic standard of limonene was also evaluated for its effect on CYP 2A6.

II. D. i. Initial Screening Assay for CYP 2A6

The assay that was used to measure inhibition of CYP 2A6 involved the hydroxylation of coumarin into 7-hydroxycoumarin. Each inhibitor was diluted by taking 5 µL of oil and dissolving it in 100 mL of DI water to make a stock solution. Conditions for the screening assay involved 25 µL of rabbit liver microsomes (source of CYP 2A6), which is approximately 1 mg/mL total protein concentration, being incubated at 37°C for 30 minutes in a reaction mixture containing 100 mM potassium phosphate buffer (pH 7.4), 80 µM of coumarin, DI water, and various amounts of each oil (ranging from 0.1 µg/mL to 3.0 µg/mL), added to give a volume of 475 µL. Each sample was vortexed and

placed in the hot water bath for one minute followed by the addition of NADPH. The reaction was initiated using 25 µL of NADPH to give a final total volume of 500 µL. Following the 30 minute incubation at 37°C the protein was precipitated out with 0.20 mL of 6 % perchloric acid and placed on ice for 10 minutes. Samples were centrifuged for 10 minutes at 3500 rpm and 460 µL of each of the clear supernants was placed in HPLC vials and analyzed by HPLC (31).

II. D. ii. HPLC Analysis

The HPLC analysis was conducted using Shimadzu's LC-20AT/ Prominence Liquid Chromatography system and the samples were detected by the SPC-20A/ Prominence UV/Vis Detector at 320 nm. Up to 100 vials were loaded into the Autosampler and a 40 µL aliquot of each sample was injected onto a 150 mm x 3.2 mm 5 micron C_{18} column with a flow rate of 0.6 mL/min and a run time of 4 minutes. The mobile phases used for this method consisted of two solutions, 100% methanol (A) and 94 % DI water, 5.0 % methanol and 1.0% acetic acid (B). The system was run with an isocratic mobile phase consisting of phases 55 % A and 45 % B. Standards were used to differentiate between the coumarin and 7-hydroxycoumarin peaks. The coumarin had a retention time of 1.97 minutes and was determined by injecting a coumarin standard solution consisting of coumarin, DI water, and 6 % perchloric acid, into the HPLC. The product, 7-hydroxycoumarin, had a retention time of 1.65 minutes and was determined by injecting an authentic standard consisting of 7-hydroxycoumarin, DI water, and 6 % perchloric acid. The 7-hydroxycoumarin peaks from each of the reaction samples were integrated to give relative activities of CYP 2A6 in rabbit liver samples.

II. D. iii. Enzyme Kinetics Assay for CYP 2A6 and K_I Determination

Conditions used for the enzyme kinetics assay involved 25 µL of rabbit liver microsomes (approximately 1 mg/mL total protein concentration) being incubated at 37°C for 30 minutes in a reaction mixture containing a range of coumarin concentrations from 2 µM to 20 µM, 100 mM potassium phosphate buffer (pH 7.4), an amount of inhibitor that gave rise to ~50 % inhibition of CYP 2A6 in the screening assays, and DI water to give a volume of 475 µL. Each sample was vortexed and placed in the 37°C water bath for one minute prior to the addition of NADPH. The reaction was initiated with the addition of 25 µL of NADPH to give a final total volume of 500 µL. A control reaction was run with each experiment that was the same as above only the inhibitor was replaced with water. Following the 30 minute incubation at 37°C the reaction was quenched with 0.20 mL of 6 % perchloric acid and placed on ice for 10 minutes to precipitate the protein. Samples were centrifuged for 10 minutes at 3500 rpm and 460 µL of the clear supernant solution was placed in HPLC vials to be analyzed by HPLC.

Michaelis-Menten plots were used in order to determine the K_I for each oil examined. Each K_I was found by plotting the V vs. [S] at a range of increasing concentration of coumarin in the presence or absence of inhibitor. The concentration of inhibitor, [I], was chosen based on the conditions of the screening experiments carried out for each oil where the conditions gave ~50 % inhibition of CYP 2A6. The Slide Write Plus (by Advanced Graphics Software, Inc.) program was used to plot the relative activity vs. concentration of coumarin. The Michaelis-Menten equation (**Equation II. 1**) was used to determine the V_{max}, $V_{max\ app}$, K_m, and $K_{m\ app}$. The K_I was calculated using the

inhibitor concentration and **Equation II. 2**. These equations were used because the $V_{max\ app}$ was within 20 % of V_{max} for of each experiment demonstrating a predominantly competitive mode of inhibition and these equations characterize a competitive model of inhibition.

III. E. Limonene Analysis

Limonene was found to be present in all of the citrus oils, and was therefore chosen as a potential candidate for the chemical inhibitor present in the oils. The GCMS analysis was conducted using a Shimadzu's GCMS-QP2010S system. GCMS was used to determine the limonene content of each of the oils. To determine the amount of limonene in each of the oils a series of dilutions of limonene in methanol were prepared and a 1.0 µL sample of each solution was injected into a Shimadzu QP2010S GCMS system to generate a limonene standard curve. The limonene peak had a retention time of 9.90 minutes and was manually integrated in order to correlate peak area with total concentration. The GCMS conditions consisted of an initial column oven temperature of 40°C that increased 1.7°C per second until it reached 280°C which was the injection temperature at 3 minutes. The injection mode was split and the total experiment was 27 minutes. The concentration in each sample was calculated based on weight, and this was plotted against the peak area given for that sample giving a standard curve for limonene. A 1.0 µL aliquot of each of the oils was dissolved in 5 mL of methanol and a 1 µL sample was injected into the GCMS. The limonene peak from each of the samples was integrated to give a relative peak area of each solution. The limonene peak area was compared with the limonene standard curve to give an estimated concentration of

limonene in each of the oils. To determine mathematically a more accurate concentration of limonene in each of the oils **Equation II. 3** (generated using the standard curve data) was used along with the relative peak area of limonene determined for each of the oils.

$$y = 18963x - 5386.3 \qquad \textbf{Equation II. 3.}$$

In **Equation II. 3 (**y) represents the relative peak area of limonene and (x) represents the concentration of limonene.

CHAPTER III

RESULTS AND DISCUSSION

III. A. Inhibition of CYP 2E1 by Citrus Essential Oils

The interaction of CYP 2E1 with citrus essential oils led to inhibition of the enzyme. This was shown using an enzymatic assay for the oxidation of p-nitrophenol to nitrocatechol with HPLC detection. The initial screening experiments were successful in demonstrating an increased inhibitory response with increasing concentration of the oil (dose-response), and in assessing relative potency of the oils with regard to CYP 2E1 inhibition. The citrus essential oil samples were initially prepared by diluting 5 µL pure oil into 100 mL of DI water. Each of the oils were included in the reaction with 50 µM p-NP in increasing concentration from 0.0 µg/mL to 3.8 µg/mL. **Figure III. 1** shows the inhibition of CYP 2E1 by the citrus essential oils of bergamot, grapefruit, lemon, lime, and mandarin. As seen in this figure, of these five oils, grapefruit oil inhibited the activity of CYP 2E1 the greatest with >50 % inhibition at a concentration lower than 2.5 µg/mL. Lemon oil also inhibited the activity of CYP 2E1 with >50 % inhibition at a concentration lower than 2.5 µg/mL, however, lemon was not as potent as grapefruit. Lime and bergamot oils inhibited >50 % at a concentration around 3.8 µg/mL. Mandarin oil was the only oil in this figure that didn't inhibit the activity of CYP 2E1 more than 50 % at concentrations as high as 3.8 µg/mL.

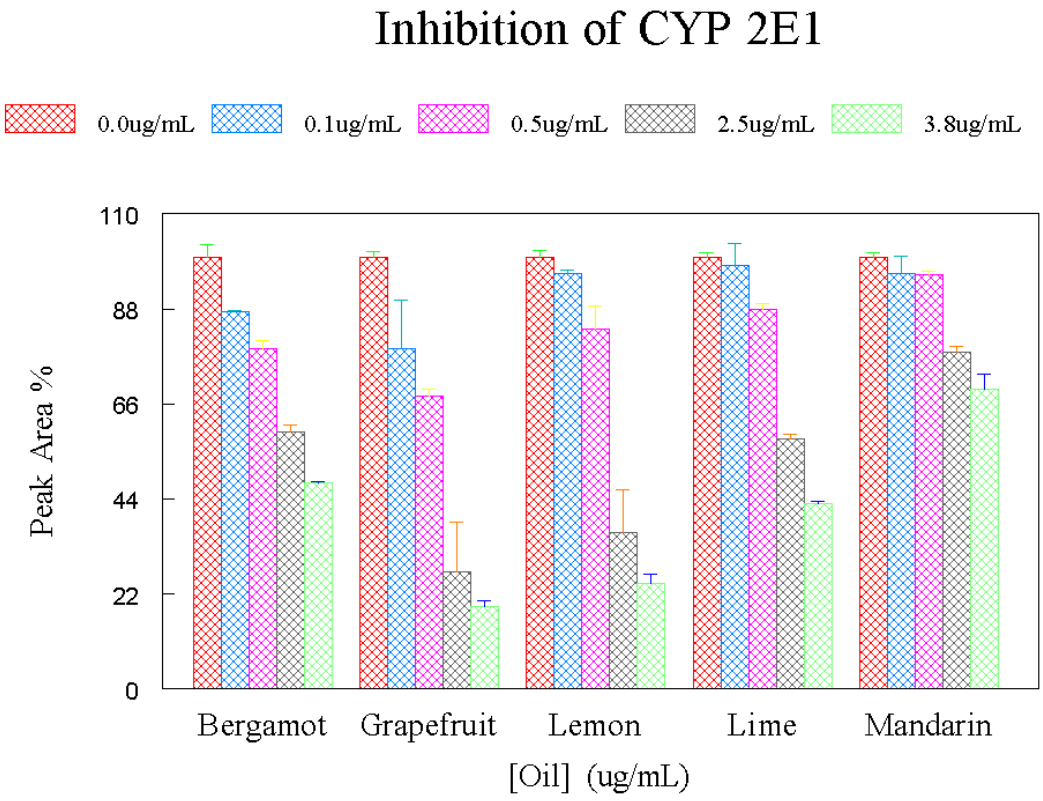

Figure III. 1: Graph of percent activity of CYP 2E1 using human liver microsomes in the presence of 50 µM p-nitrophenol and different essential oils from 0.0 µg/mL to 3.8 µg/mL.

Since the main compound found in grapefruit oil is limonene it was proposed that limonene might be the cause of the inhibition of the activity of CYP 2E1. Literature results of the limonene content found in these citrus essential oils, **Table I. 1**, showed that limonene is found in all of the citrus essential oils used for inhibition studies for CYP 2E1. **Figure III. 2** shows the inhibition of CYP 2E1 by the citrus essential oils of neroli, orange, petitgrain, tangerine, and limonene. As seen in this figure, of these five oils, orange oil inhibited the activity of CYP 2E1 the greatest with >50 % inhibition at a

concentration lower than 2.5 µg/mL. Tangerine oil, petitgrain oil, and neroli oil all inhibited the activity of CYP 2E1 by >50 % at concentrations lower than 2.5 µg/mL, however, orange oil was the most potent. As seen in **Figure III. 2**, limonene did not inhibit the activity of CYP 2E1 by 50 % even at the highest concentrations of 3.8 µg/mL. Based on initial comparison of the screening data for all nine of the citrus essential oils, grapefruit oil appeared to be the most potent oil inhibiting the activity of CYP 2E1 by ~70 % at concentrations lower than 2.5 µg/mL. Mandarin oil was found to be the least potent oil to inhibit CYP 2E1 activity only showing about 30 % inhibition of CYP 2E1 activity at a concentration of 3.8 µg/mL. Given the occurrence of limonene in all of the citrus oils studied, we sought to link the inhibition of CYP 2E1 by the citrus oils to the presence of this monoterpeniod compound. To make this correlation, a standard curve was prepared for limonene using GCMS as described later in the chapter.

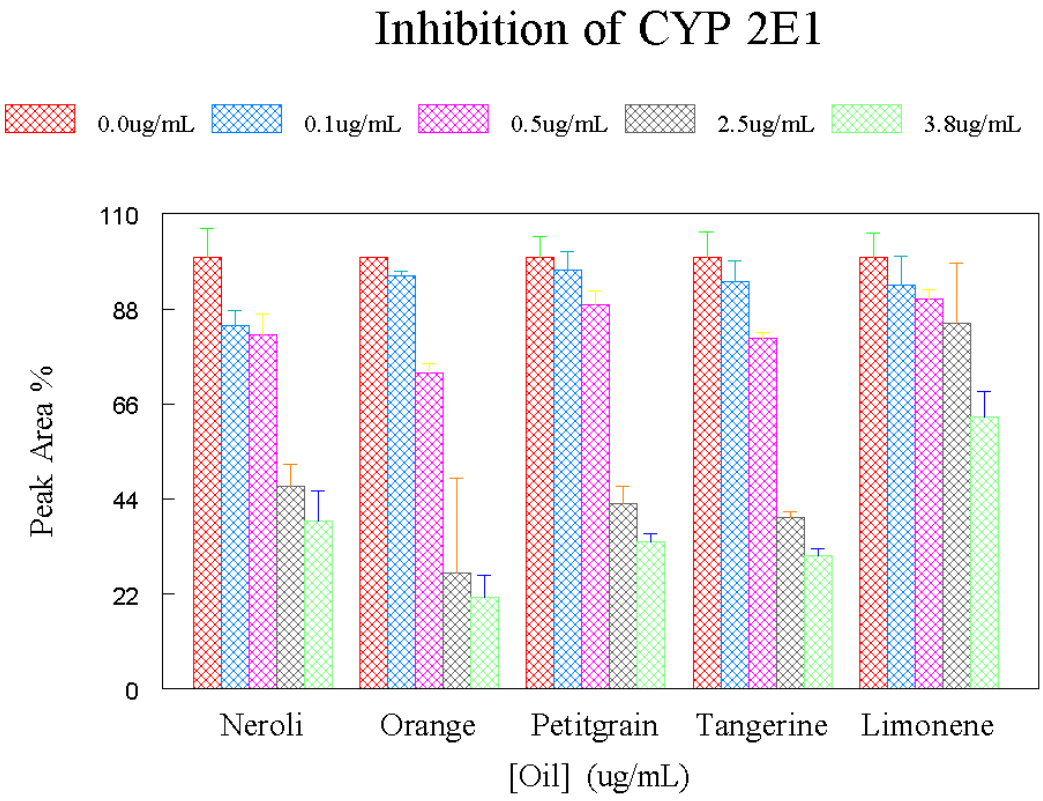

Figure III. 2: Graph of percent activity of CYP 2E1 using human liver microsomes in the presence of 50 µM p-nitrophenol and different essential oils from 0.0 µg/mL to 3.8 µg/mL.

III. A. i. Enzyme Kinetics Analysis

A more precise characterization of the inhibitory effects of there citrus essential oils on the activity of CYP 2E1 was achieved via kinetics analysis using the Michaelis-Menten model of enzyme kinetics and inhibition. The kinetics experiments were carried out using 5 different p-NP concentrations ranging from 20 µM to 160 µM in the presence and absence of inhibitor in duplicate or triplicate to ensure reproducible. The concentration of oil selected for each experiment was based on the results of the initial screening studies. A concentration was selected where ≥ 50 % inhibition was observed

under the standard conditions used for screening. Human microsomes were incubated with one of the nine oils examined and p-NP using different concentrations of substrate ranging from 20 µM to 160 µM. The relative activities (as determined by integration of the peak area for the product nitrocatechol) were plotted against the concentration of p-NP as in a Michaelis-Menten model. Based on the observation that the V_{max} for the control experiments and those with inhibitor present were virtually the same, a competitive model of inhibition was used to calculate a K_I for each of the nine oils examined (**Table III. 1**), in order to generate a quantitative measure of the inhibition.

Essential Oil	K_I (µg/mL)	Error (µg/mL)	K_m	$K_{m\ app}$	V_{max}	$V_{max\ app}$
Grapefruit	9	± 1.6	14	36	92	118
Orange	8	± 2.5	15	40	118	104
Tangerine	4.3	± 0.20	14	55	97	106
Mandarin	7	± 1.0	15	82	99	102
Lemon	8	± 0.34	16	43	146	118
Lime	10	± 2.5	18	82	99	88
Bergamot	6.4	± 1.1	10	64	92	103
Neroli	14	± 2.4	17	48	123	105
Petitgrain	7.6	± 0.43	15	64	106	119

Table III. 1: Averaged K_I values and error values calculated for CYP 2E1 inhibition activity by the nine citrus essential oils examined. Also included are K_m, $K_{m\ app}$, V_{max} and $V_{max\ app}$ values for all of the oils.

Of the nine oils examined using the Michaelis-Menten model, tangerine oil was found to be the most potent inhibitor based on its calculated K_I. To illustrate how the values in

Table III. 1 were obtained, sample kinetics plots for tangerine and neroli oil are shown in **Figures III. 3 and III. 4**. **Figure III. 3** shows a representative experiment shown as a Michaelis-Menten plot for tangerine oil. Based on the data shown in the Michaelis-Menten plot (**Figure III. 3**), a V_{max} and K_M were calculated in the absence and presence of tangerine oil. Based on the observation that V_{max} was unaffected, the competitive model of inhibition was used to calculate a K_I of 4.04 μg/mL for tangerine oil. For example, K_m was 14.48 and $K_{m\ app}$ was 58.95. The ratio of K_m / $K_{m\ app}$ was set equal to α and substituted into **Equation III. 1**.

$$\alpha = 1 + [I] / K_I \qquad \textbf{Equation III. 1.}$$

Of the nine oils examined during screening neroli was found to be the least potent inhibitor based on Michaelis-Menten experiments. Therefore the corresponding data for this α are also included. **Figure III. 4** shows a representative experiment shown as a the Michaelis-Menten plot for neroli oil. Based on the data shown in the Michaelis-Menten plot (**Figure III. 4**), a V_{max} and K_m were calculated in the absence and presence of neroli oil. Once again V_{max} was unaffected by the presence of the oil, whereas a significant effect was observed on K_m, the competitive model of inhibition was used to calculate a K_I of 11.48 μg/mL for neroli oil.

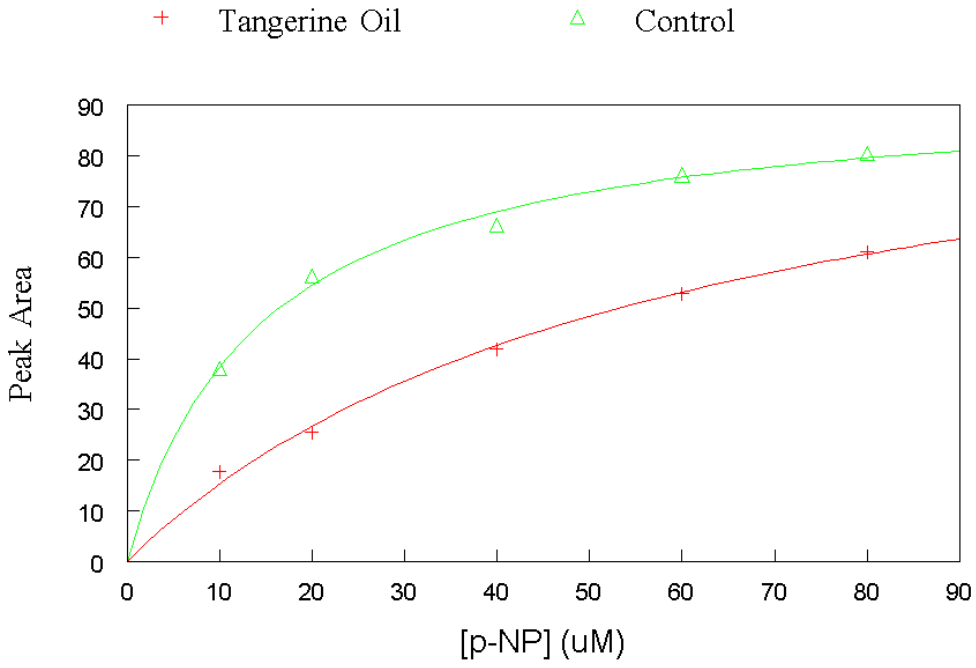

Figure III. 3: Plot of area vs. p-nitrophenol (µM) concentration in the presence (pluses) and absence (triangles) of tangerine oil. Reactions contained inhibitor, human liver microsomes, a range of substrate concentrations from 20 µM to 160 µM, and NADPH.

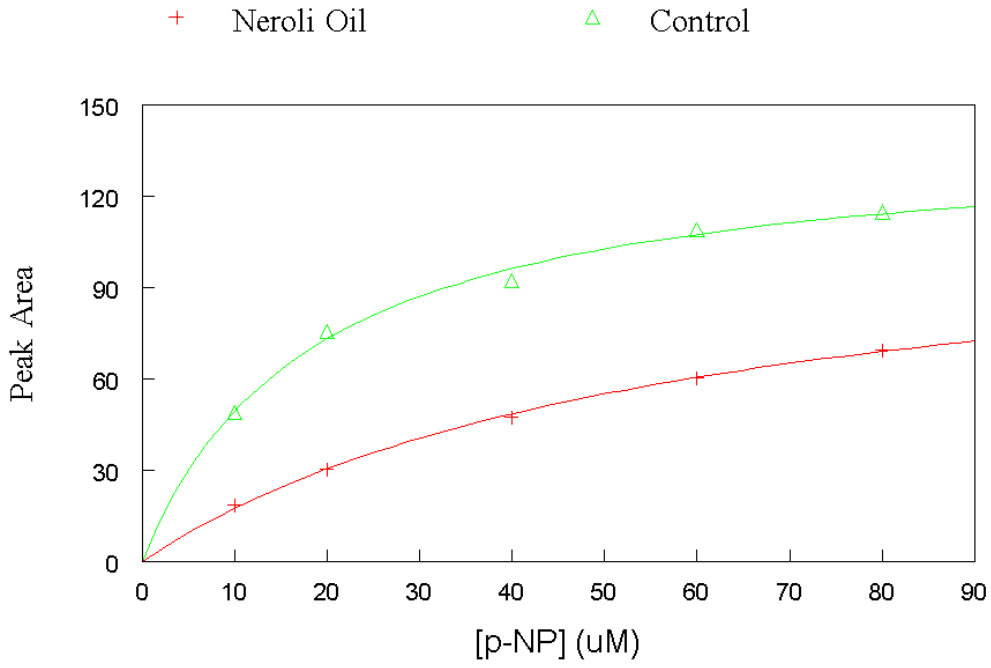

Figure III. 4: Plot of area vs. p-nitrophenol (µM) concentration in the presence (pluses) and absence (triangles) of neroli oil. Reactions contained inhibitor, human liver microsomes, a range of substrate concentrations from 20 µM to 160 µM, and NADPH.

III. B. Inhibition of CYP 3A6 by Citrus Essential Oils

The importance of CYP 3A4 in the metabolism of pharmaceuticals prompted the current investigation into the inhibitory effect of citrus oils on this CYP 450 isoform. Ortiz de Montellano *et al* (13) have reported that 30 % of all drugs are metabolized by human CYP 3A4, and the interaction between CYP 3A4 and grapefruit juice, and the potential for adverse drug interactions are well documented (13). The interaction of CYP 3A6 with citrus essential oils lead to very poor inhibition of the enzyme. This was shown

using the enzymatic assay for the oxidation of nifedipine to oxidized nifedipine with HPLC detection. Our initial efforts focused on development of an assay to determine the optimal conditions for measuring activity of CYP 3A6 in rabbit liver microsomes (source of CYP 3A6). The rabbit liver was chosen as a model to look at inhibition of 3A family enzymes. The rabbit liver CYP 3A6 is closely related to the human CYP 3A4.

The method reported in the literature for the CYP 3A-dependent nifedipine oxidation involved a solvent extraction step prior to HPLC analysis, which is time consuming and difficult for high through-put analysis (6). We sought to improve this assay by finding a way to eliminate the extraction step, which would make the assay faster and easier to use. Several different quenching methods were evaluated in an attempt to eliminate extraction and streamline the assay. Initially, 35 % trichloro acetic acid was used to terminate the CYP450 reaction, however the data observed for the samples were somewhat inconsistent. Next, the addition of a 6.0 % perchloric acid solution was used to quench the reaction and the data observed for these samples were similar to those obtained using the extraction method. As a result, using 6.0 % perchloric acid to quench the reactions followed by protein precipitation and centrifugation gave better reproducibility and was less time consuming than the extraction method. Therefore, this non-extraction method was adopted for all subsequent studies.

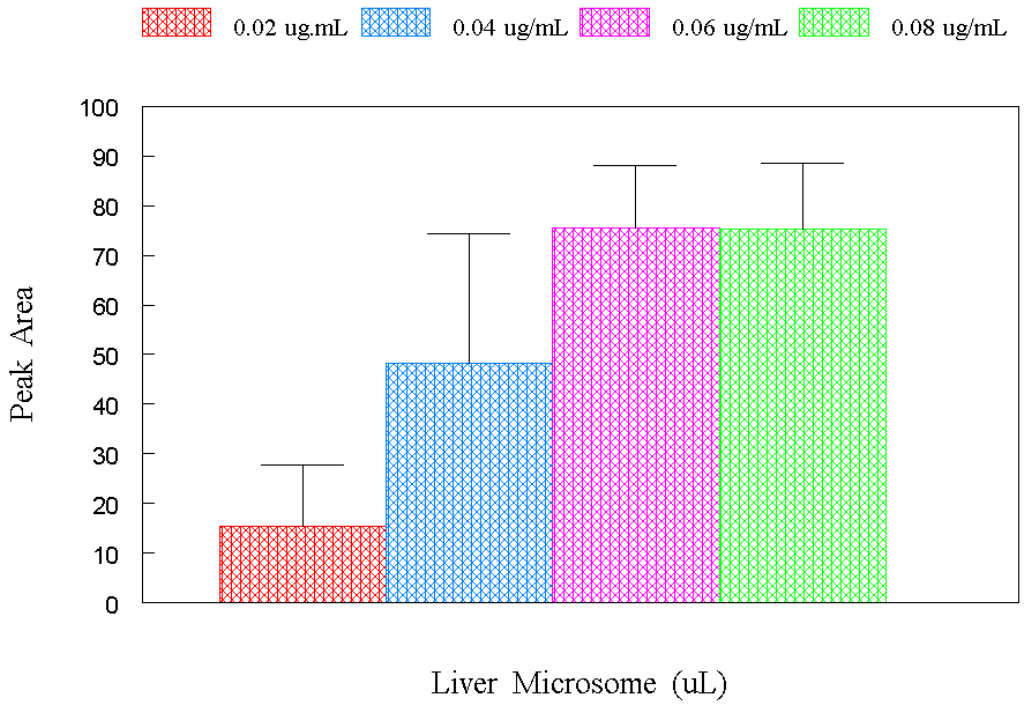

Figure III. 5: Graph of the amount of oxidized nifedipine produced by rabbit liver microsomes, a source of CYP 3A6, with increasing amounts of microsomes from 0.02 µg/mL to 0.08 µg/mL, 10 µM nifedipine, and a NADPH-regenerating system.

Figure III. 5 shows the amount of oxidized nifedipine that was produced when the reaction contained either 0.02 µg/mL, 0.04 µg/mL, 0.06 µg/mL, or 0.08 µg/mL of rabbit liver microsomes (approximately 1 mg/mL total protein concentration). The relationship between the amount of oxidized nifedipine produced and the amount of microsomes present in the reaction is approximately linear up to 0.06 mg/mL of microsomes, suggesting that above 0.06 mg/mL one of the reaction components may have been fully consumed.

High Performance Liquid Chromatography was used to analysis each sample. All samples were run on a 150 mm x 3.2 mm 5 micron C_{18} column and detection was set at a wavelength of 340 nm with the flow rate set at 0.6 mL/min and a run time of 8 minutes. To analyze the amount of oxidized nifedipine by CYP 3A6 several methods were examined using HPLC. Several different mobile phases were evaluated to establish the best chromatogram results for the separation of oxidized nifedipine and nifedipine. The two solvent system mobile phases that were used to evaluate the activity of CYP 3A6 consisted of 100 % methanol (A) and 0.5 % acetic acid in DI water (B). The first mobile phase tested consisted of a 50/50 mixture of A and B, but product and reactant peaks were not sharp and were too close together. The peaks were joined together and a proper integration of the oxidized nifedipine peak was not possible. The mobile phases were then changed to a 60/40 solution of A and B, respectively, and the peaks were well resolved and easily integrated.

Figure III. 6 shows an HPLC chromatogram of both nifedipine and oxidized nifedipine standards. The nifedipine standard contained 10 μM nifedipine, DI water, and 2 % perchloric acid. The peak seen at about 290 seconds was determined to be nifedipine. The peak with the retention time around 200 seconds was observed for the oxidized nifedipine standard which contained an authentic sample of oxidized nifedipine, DI water, and 2 % perchloric acid. This peak was also observed in reactions with rabbit liver microsomes, nifedipine and NADPH was used to quantify CYP 3A6 activity in the

rabbit microsomes.

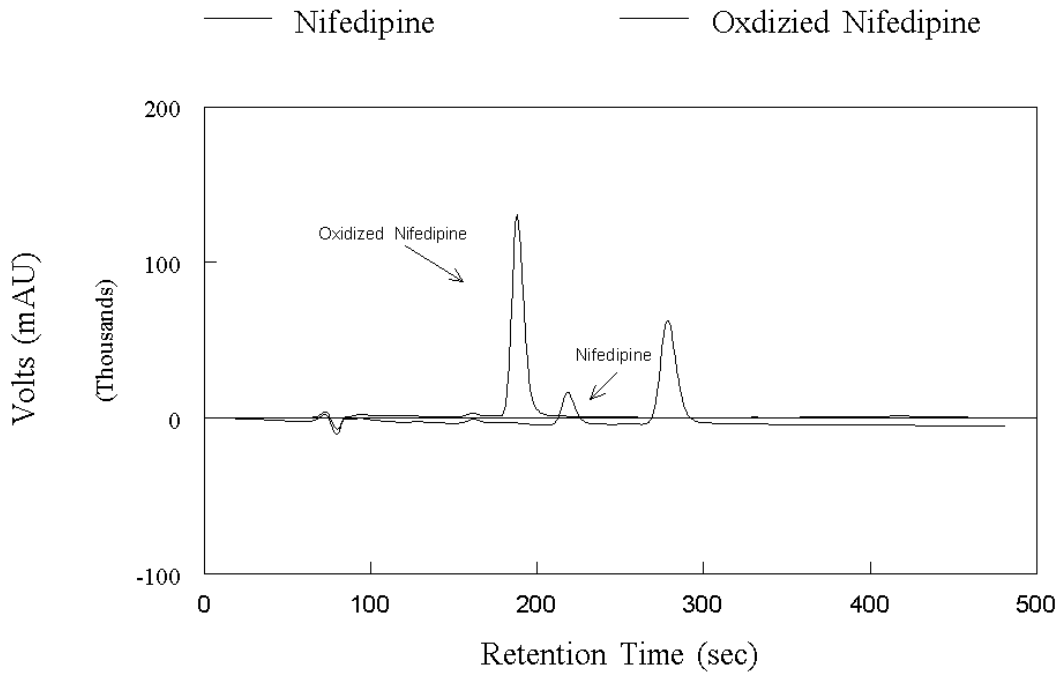

Figure III. 6: Oxidized nifedipine and nifedipine standards HPLC chromatograms containing either oxidized nifedipine or 10 µM nifedipine and DI water and 2 % perchloric acid, but lacked NADPH. The peak at 190 sec. was identified as oxidized nifedipine. The smaller peak at 270 sec. was identified as nifedipine.

Initially, as with the CYP 2E1 assay, each oil was screened for its ability to inhibit CYP 3A6. The screening experiment was successful in producing consistent results for all the essential oils examined. Each citrus essential oil was examined by visual inspection of the dose response data in either duplicate or triplicate to ensure reproducibility. The citrus essential oils were initially diluted by taking 5 µL and dissolving it in 100 mL of DI water. Each of the oils were included in the reaction with

10 µM nifedipine in increasing concentration from 0.0 µg/mL to 3.0 µg/mL. **Figure III. 7** shows the inhibition of CYP 3A6 by the citrus essential oils of bergamot, grapefruit, lemon, lime, and mandarin. As seen in this figure, of these five oils, lemon oil inhibited the activity of CYP 3A6 the greatest but did not reach >50 % inhibition at concentrations as high as 3.0 µg/mL. Mandarin and bergamot oils also inhibited the activity of CYP 3A6 however >50 % inhibition at concentrations as high as 3.0 µg/mL was not reach. None of the five oils shown in this figure reached 50 % inhibition of CYP 3A6 activity at concentrations as high as 3.0 µg/mL. Interestingly, for all of the oils except lime, there appeared to be a modest increase in activity at the lowest concentration of oil, followed by a return to 100 % or slight inhibition at the higher concentrations. Clearly, based on these findings, none of the first 5 oils tested appeared to interact strongly with the rabbit CYP 3A6 isoform.

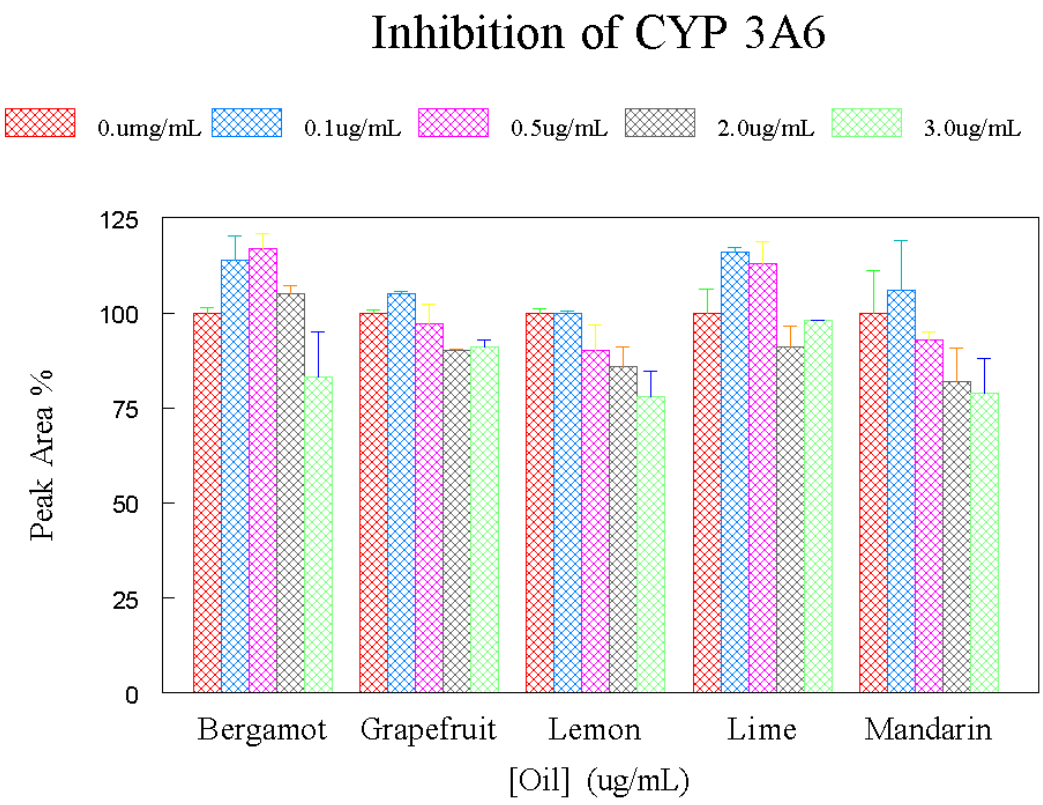

Figure III. 7: Graph of percent activity of CYP 3A6 using rabbit liver microsomes in the presence of 10 µM nifedipine and different essential oils from 0.0 µg/mL to 3.0 µg/mL.

Figure III. 8 shows the inhibition of CYP 3A6 by the citrus essential oils of neroli, orange, petitgrain, tangerine, and limonene. Orange oil was the only oil that we were unable to obtain reproducible data for. The other four oils in the figure showed very little inhibition on the activity of CYP 3A6, not reaching 50 % inhibition at concentrations as high as 3.0 µg/mL. Again, the oil of neroli appeared to stimulate activity at the lowest concentration. Several explanations may account for this modest stimulation. For example, it has been reported that radical scavenging can affect the activity of CYP 3A4

(27). It is thought that antioxidants interact with the free radical chain of oxidation by donating a hydrogen atom and forming a stable product. Basavaraj Girennavar *et al* have shown that bergaptol and geranylcoumarin, isolated from grapefruit juice, act as radical scavengers when tested against CYP 3A4 enzymes.

The results that were observed for the inhibition of CYP 3A6 activity experiments suggested that the citrus essential oils tested had only modest effect on the activity of CYP 3A4. The general lack of inhibition of CYP 3A6 by the oils could be due to the small size of most of the oils constituents, as monoterpenes, relative to the size of CYP 3A6's active site. This is interpreted to suggest that citrus essential oils would gave no significant impact on the human CYP 3A4 and thus should pose no threat of adverse drug interactions.

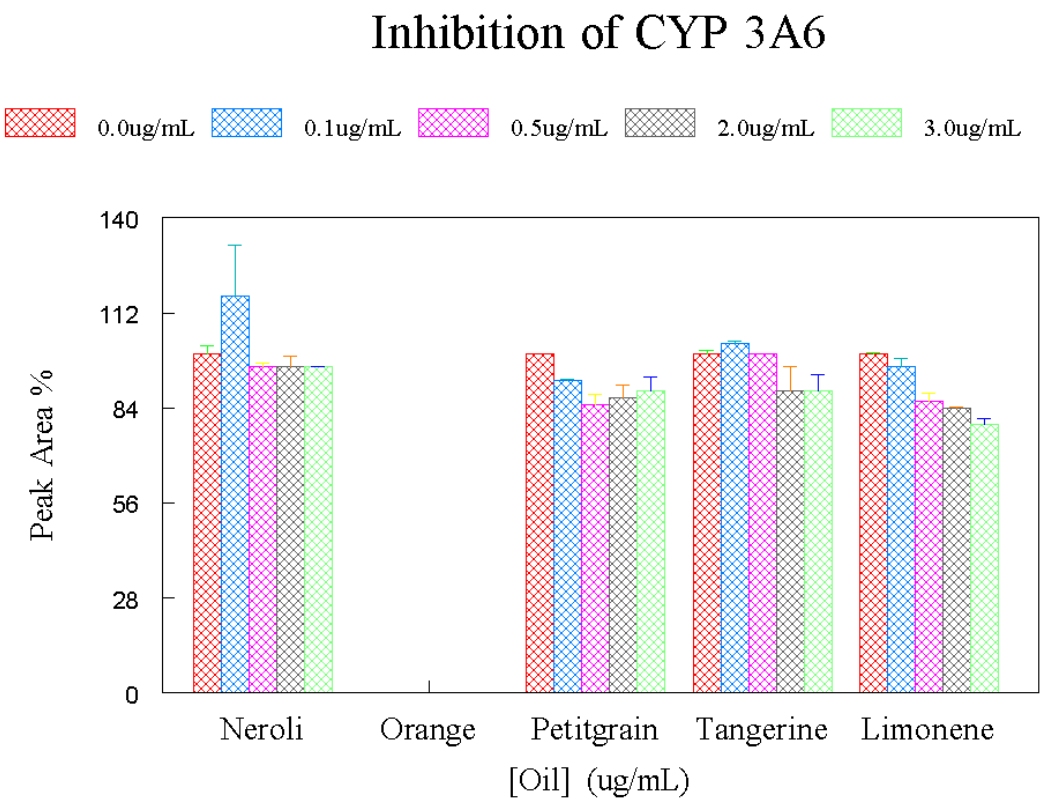

Figure III. 8: Graph of percent activity of CYP 3A6 using rabbit liver microsomes in the presence of 10 μM nifedipine and different essential oils from 0.0 μg/mL to 3.0 μg/mL.

III. C. Inhibition of CYP 2A6 by Citrus Essential Oils

The interaction of CYP 2A6 with citrus essential oils led to relatively strong inhibition of the enzyme. This was shown using an enzymatic assay for the hydroxylation of coumarin into 7-hydroxylation with HPLC detection. This assay was developed in our lab for the purpose of high throughput HPLC analysis of CYP 2A6 inhibitors. **Figure III. 9** shows an HPLC chromatogram of both coumarin and 7-hydroxycoumarin combined. The coumarin standard contained 80 μM coumarin, DI

water, and 2 % perchloric acid. The peak seen at about 115 sec. was determined to be coumarin. The peak with the retention time around 95 sec. was observed for the reaction mixture that was the 7-hydroxycoumarin standard which contained 1.0 μM 7-hyrdoxycoumarin, DI water, and 2 % perchloric acid.

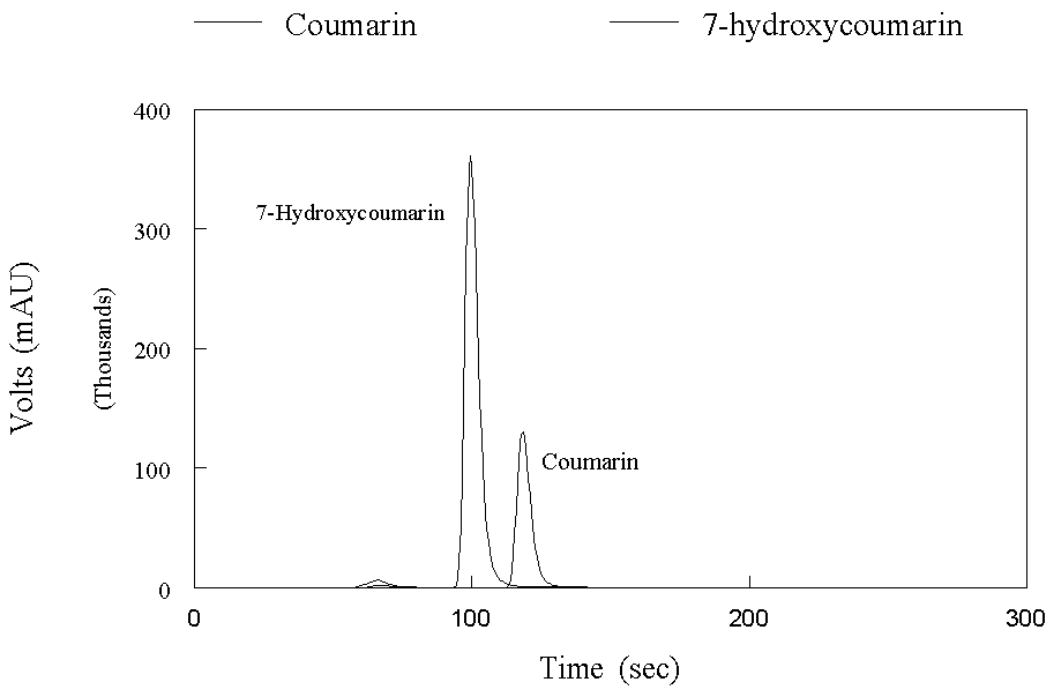

Figure III. 9: 7-Hydroxycoumarin and coumarin standards HPLC chromatograms containing either 1.0 mM 7-hydroxycoumarin or 1.0 mM nifedipine and DI water and 6 % perchloric acid, but lacked NADPH. The peak at 95 sec. was identified as 7-hydroxycoumarin. The smaller peak at 115 sec. was identified as coumarin.

The interaction of CYP 2A6 with certain citrus essential oils led to relatively potent inhibition of the enzyme when compared with CYP 3A4. This was shown using an initial screening of the oils for their inhibition of the enzymatic activity of rabbit liver

microsomes in the hydroxylation of coumarin into 7-hydroxycoumarin. The initial screening experiment gave reproducible results for all the essential oils examined when carried out in duplicate or triplicate. Each citrus essential oil was examined initially by visual inspection of the dose response. The citrus essential oils were initially diluted by taking 5 µL of the oil and dissolving it in 100 mL of DI water. Each of the oils were included in the reaction with 80 µM coumarin in increasing concentration from 0.0 µg/mL to 3.0 µg/mL.

To illustrate the effect that lime and bergamot oil have on the activity of CYP 2A6, chromatograms from the screening experiments of the two oils are presented in **Figure III. 10.** These chromatograms represent the initial inhibition screening data used for the screening of the lime oil conducted on CYP 2A6 activity. In order to better visualize the effect that lime oil had on the activity of CYP 2A6 only the 7-hyrdoxycoumarin peaks are shown in the figure. The control line represents the control experiment in which no inhibitor was present. The 0.1 µg/mL line is representative of the data when the inhibitor concentration was 0.1 µg/mL, the 0.5 µg/mL line if when the inhibitor concentration was at 0.5 µg/mL, the 2.0 µg/mL line is when the inhibitor concentration was at 2.0 µg/mL, and the 3.0 µg/mL line is when the inhibitor concentration was at 3.0 µg/mL. As seen in this figure, lime oil showed a >50 % inhibition of the activity of CYP 2A6 at only 0.5 µg/mL. **Figure III. 11** shows a chromatogram of the initial inhibition screening data used for the screening inhibition of the bergamot oil conducted on CYP 2A6 activity. Again, to better visualize the effect that bergamot oil had on the activity of CYP 2A6 only the 7-hyrdoxycoumarin (product)

peaks are shown in the figure. The control line represents the control experiment in which no inhibitor was present. The 0.1 µg/mL line is representative of the data when the inhibitor concentration was 0.1 µg/mL, the 0.5 µg/mL line if when the inhibitor concentration was at 0.5 µg/mL, the 2.0 µg/mL was when the inhibitor concentration was at 2.0 µg/mL, and the 3.0 µg/mL line was when the inhibitor concentration was at 3.0 µg/mL. As with bergamot, lime oil shows >50 % inhibition of the activity of CYP 2A6 at only 0.5 µg/mL.

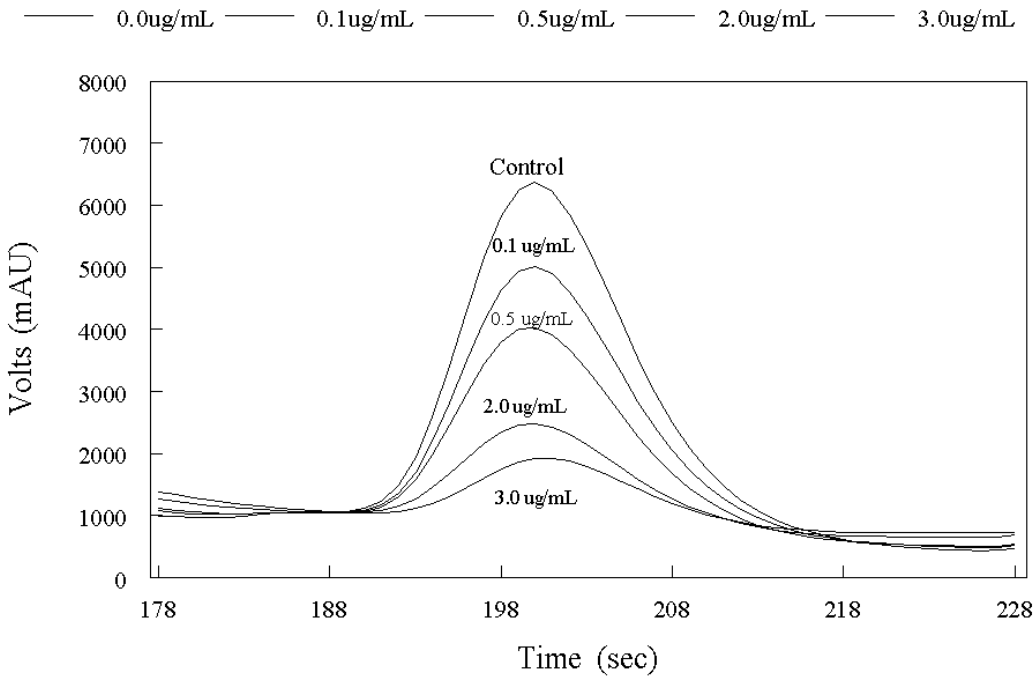

Figure III. 10: Chromatogram of the screening data used for the initial screening inhibition experiment of lime oil on CYP 2A6 activity. Reactions contained rabbit liver microsomes, DI water, 80 µM coumarin, a range of inhibitor from 0.0 µg/mL , 0.1 µg/mL, 0.5 µg/mL, 2.0 µg/mL, and 3.0 µg/mL, and NADPH.

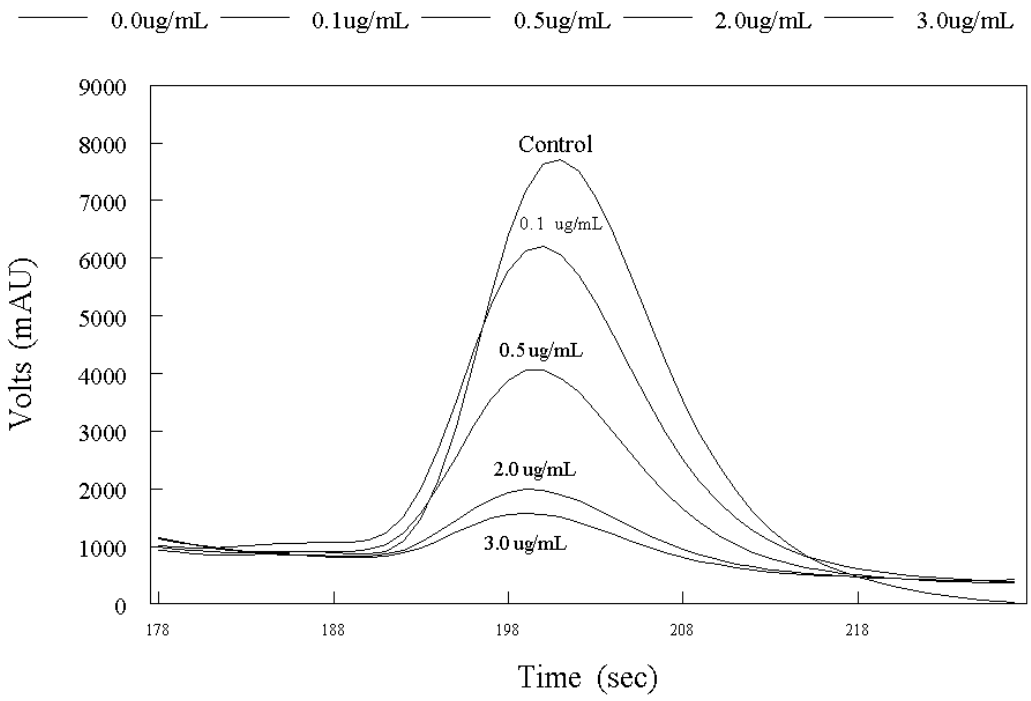

Figure III. 11: Chromatogram of the screening data used for the initial screening inhibition experiment of bergamot oil on CYP 2A6 activity. Reactions contained rabbit liver microsomes, DI water, 80 µM coumarin, a range of inhibitor from 0.0 µg/mL, 0.1 µg/mL, 0.5 µg/mL, 2.0 µg/mL, and 3.0 µg/mL, and NADPH.

Figure III. 12 shows the inhibition of CYP 2A6 by the citrus essential oils of bergamot, grapefruit, lemon, lime, and mandarin. As seen in this figure, of these five oils, lime oil inhibited the activity of CYP 2A6 the greatest with >50 % inhibition at a concentrations as low as 0.5 µg/mL. Bergamot oil also inhibited the activity of CYP 2A6 at a concentration of 0.5 µg/mL. Mandarin oil and grapefruit oil were the only oils, shown in this figure, that did not inhibit the activity of CYP 2A6 by 50 % inhibition at a

concentration as high as 3.0 µg/mL. Lemon oil inhibited the activity of CYP 2A6 by 50 % at a concentration around 1.3 µg/mL.

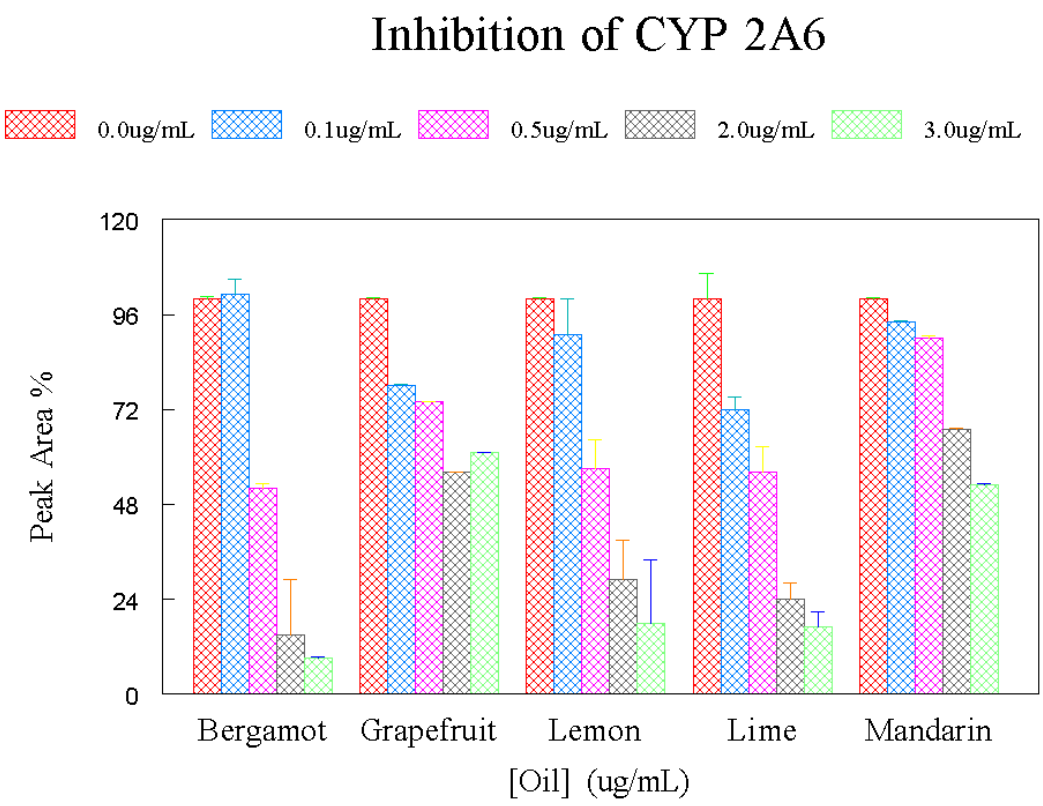

Figure III. 12: Graph of percent activity of CYP 2A6 using rabbit liver microsomes, source of CYP 2A6, in the presence of 80 µM coumarin and different essential oils from 0.0 µg/mL to 3.0 µg/mL.

Figure III. 13 shows the inhibition of CYP 2E1 by the citrus essential oils of neroli, orange, petitgrain, tangerine, and limonene. As seen in this figure, petitgrain oil inhibited the activity of CYP 2A6 the greatest with >50 % inhibition at a concentration of 2.0 µg/mL. Neroli oil and orange oil showed moderately good inhibition of the activity of

CYP 2A6 with 50 % inhibition at a concentration of 1.3 µg/mL however they were not as potent of an inhibitor of CYP 2A6 as bergamot oil and lime oil. Tangerine oil was the least potent inhibitor in this figure, showing little inhibition by only reaching >50 % inhibition of CYP 2A6 activity at a concentration of about 2.5 µg/mL. Limonene showed moderately good inhibition of CYP 2A6 activity, reaching >50 % inhibition at a concentration of about 1.3 µg/mL. All of these observations point to bergamot and lime oil being the most potent inhibitors of CYP 2A6.

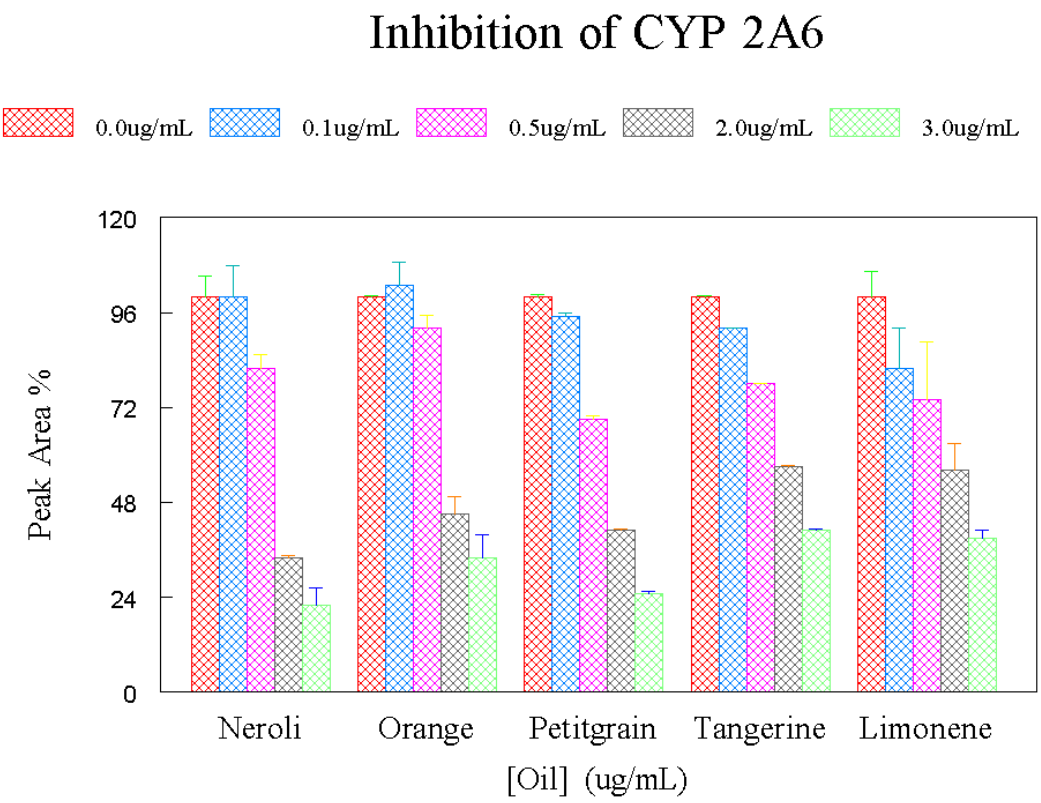

Figure III. 13: Graph of percent activity of CYP 2A6 using rabbit liver microsomes, source of CYP 2A6, in the presence of 80µM coumarin and different essential oils from 0.0 µg/mL to 3.0 µg/mL.

III. C. i. Enzyme Kinetics Analysis for CYP 2A6

To better characterize the effects of the bergamot and lime citrus essential oils on the activity of CYP 2A6 each of them were examined using the Michaelis-Menten model of enzyme kinetics and inhibition. The experiments were carried out in the presence and absence of inhibitor in duplicate or triplicate for demonstration of reproducibility. Rabbit liver microsomes, the source of CYP 2A6, were incubated with one of oils, diluted 5 µL into 100 mL of DI water, and 80 µM coumarin using different concentrations of substrate ranging from 0.01 µM to 0.10 µM. The amount of inhibitor used for each oil was determined using the screening assay for that given oil where it gave ~50 % inhibition of CYP 2A6 activity, which in both cases was 0.5 µg/mL. The relative activities were plotted against the concentration of coumarin as in a Michaelis-Menten model. Based on the observation that the V_{max} between the control experiment and the experiment with inhibitor present was unaffected, a competitive model of inhibition and **Equation II. 1** and **Equation II. 2** were used to calculate a K_I for each the oils examined (**Table III. 2**). Since bergamot and lime were more potent than the other oils used in the screening study, only these two oils were evaluated for K_I determination.

Essential Oil	K_I µg/mL
Bergamot	0.81
Lime	1.4

Table III. 2: K_I values calculated for CYP 2A6 inhibition activity by bergamot and lime citrus essential oils.

Of the two oils examined bergamot oil was found to be the most potent inhibitor based on the kinetics data. **Figure III. 14** shows a representative experiment shown as a Michaelis-Menten plot for lime oil. Based on the data shown in this plot (**Figure III. 14**), a V_{max} and K_M were calculated in the absence and presence of lime oil. Once again V_{max} appeared to be unaffected so the competitive model of inhibition and **Equation II. 1** and **Equation II. 2** were used to calculate a K_I of 1.4 μg/mL for lime oil. The essential oil lime was found to be a less potent inhibitor than bergamot oil based on Michaelis-Menten experiment shown in **Figure III. 15**. Based on the data in this Michaelis-Menten plot (**Figure III. 15**), a V_{max} and K_M were calculated in the absence and presence of bergamot oil. The observed V_{max} was once again unaffected by the presence of the oil and the competitive model of inhibition used to calculate a K_I of 0.81 μg/mL for bergamot oil.

As stated previously, tobacco use has been associated with different types of cancers for quite some time. Cancers of the lung, larynx, mouth, esophagus, kidneys, and urinary tract have all been linked to tobacco use. It has been shown that CYP450 enzymes are able to metabolize tobacco carcinogens into DNA-binding metabolites (22). CYP 2A6 enzymes are the main catalyst involved in the metabolism of nicotine to cotinine via 3'-hyrdoxylation (13). The inhibition of CYP 2A6 has recently been identified as a possible therapeutic approach to smoking cessation, therefore giving significant importance to bergamot and lime oils and the compounds found in them. Bergamot and lime oils both contain the compound limonene and also both contain the compounds geranial and linalol. It is proposed that another compound found in these oils

may react with limonene to cause the inhibition of CYP 2A6 activity since both oils presented low concentrations of limonene compared to the other oils examined.

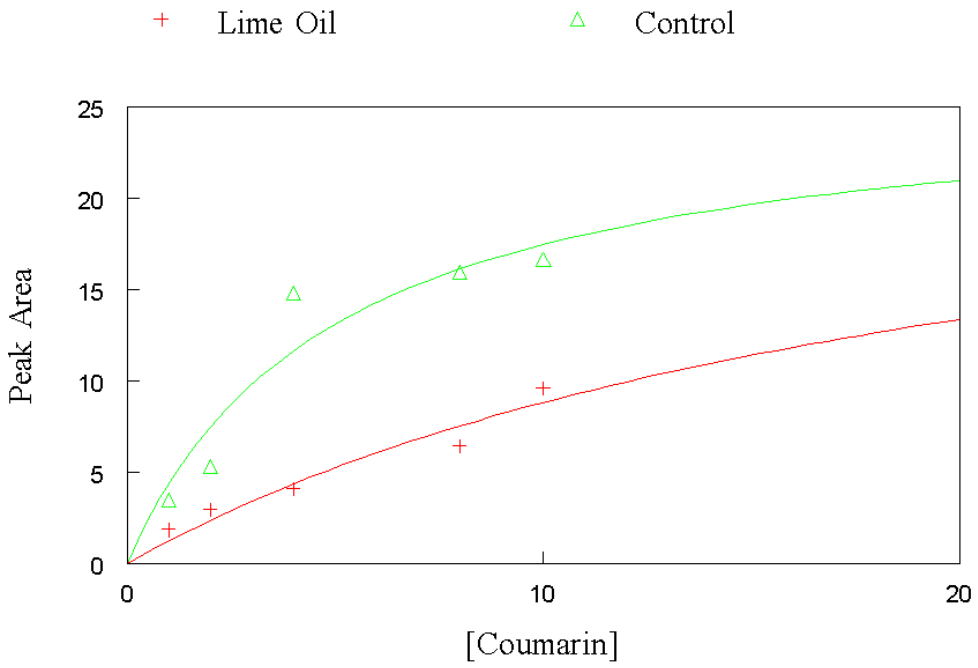

Figure III. 14: Plot of area vs. coumarin concentration, best representative, in the presence (pluses) and absence (triangles) of lime oil (0.50 µM). Reactions contained inhibitor, rabbit liver microsomes, a range of substrate concentrations from 0.01 mM to 0.10 mM, and NADPH.

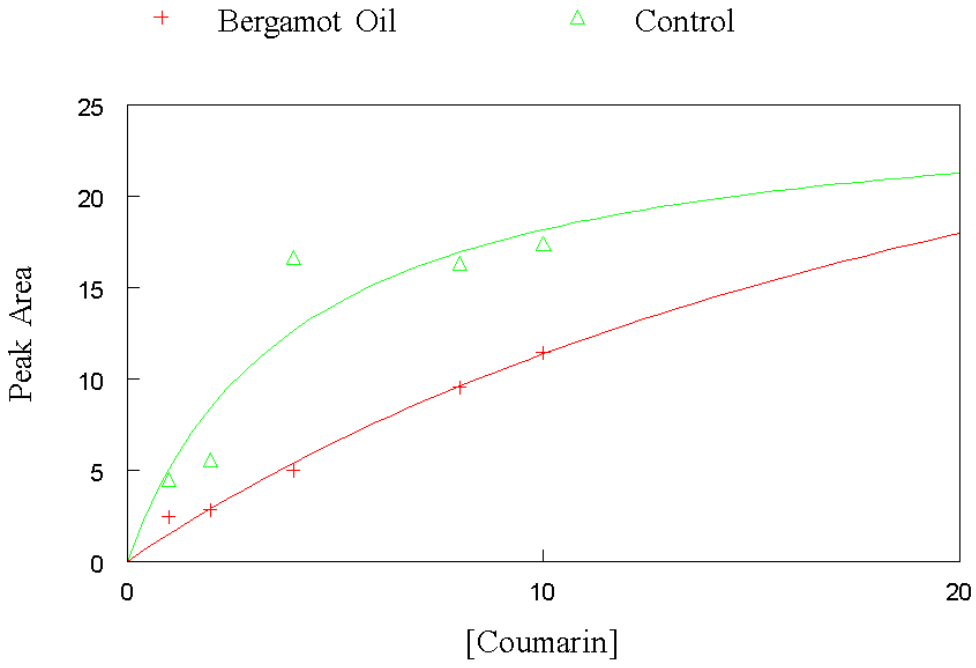

Figure III. 15: Plot of area vs. coumarin concentration, best representative, in the presence (pluses) and absence (triangles) of bergamot oil (0.50 µM). Reactions contained inhibitor, rabbit liver microsomes, a range of substrate concentrations from 0.01 mM to 0.10 mM, and NADPH.

III. D. Limonene Analysis

The GCMS analysis was conducted using a Shimadzu's GCMS-QP2010S system. GCMS was used to determine the limonene content of limonene standards and each of the oils examined. To determine the amount of limonene in each of the oils a series of dilutions of limonene in methanol were prepared and a 1 µL sample of each solution was injected into a Shimadzu GCMS system to generate a limonene standard curve (**Figure III. 16**). The limonene peak had a retention time of 9.90 minutes and was able to be

manually integrated using parameters based on its molecular weight of 136 g/mol to give a total ion concentration of limonene in each sample. Based on the weight of a 10 µL sample of the limonene used in the experiments the concentration in each sample was determined and plotted against the average peak area determined for that sample. **Figure III. 16** shows the plot of the average limonene peak area vs. the concentration of limonene in each dilution along with the data collected for each of the nine oils examined. The average limonene peak area was plotted onto the limonene standard curve to give an estimated concentration of limonene in each of the oils (**Figure III. 16**). Each oil is represented by a different number in the figure, bergamot is 1, grapefruit is 2, lemon is 3, lime is 4, mandarin is 5, neroli is 6, orange is 7, and tangerine is 8. Petitgrain oil was the only oil that a limonene peak was unable to be detected in which is expected when compared with the literature results of only have about a 1-2% limonene content (**Table I. 1**).

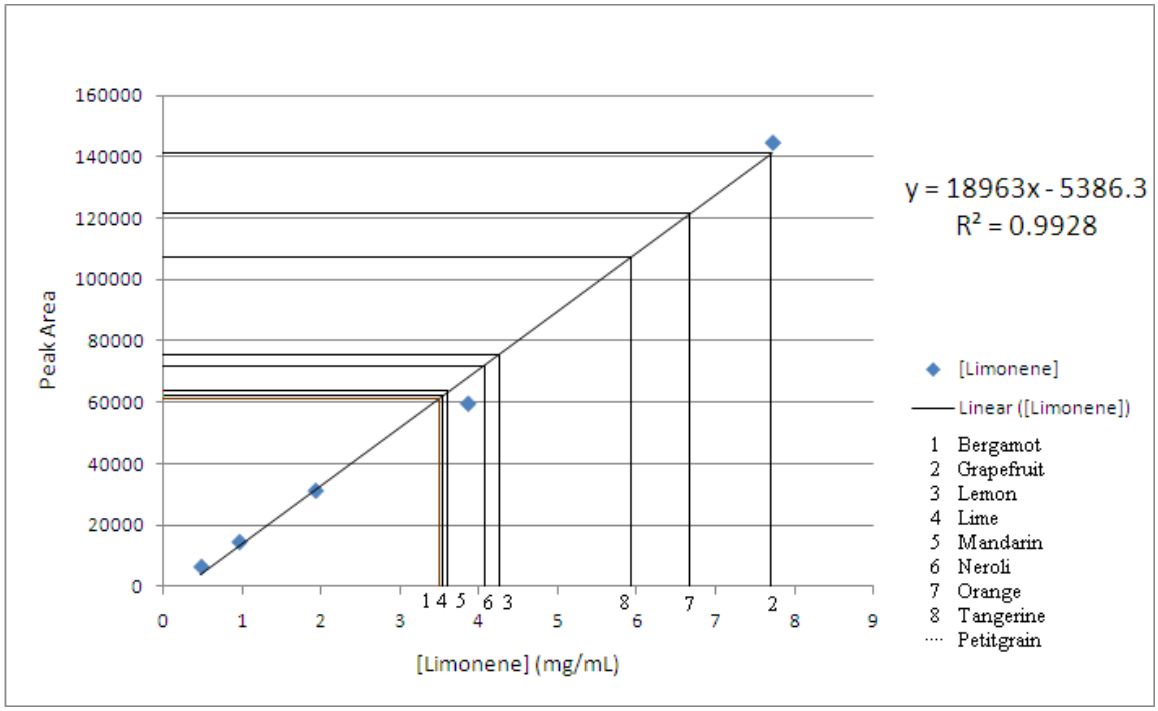

Figure III. 16: Limonene standard curve showing the average peak area of limonene content in each standard dilution vs. total calculated limonene content. Oils are integrated into plot showing an estimated value for total limonene content in each oil, bergamot (1), grapefruit (2), lemon (3), lime (4), mandarin (5), neroli (6), orange (7), and tangerine (8).

To determine mathematically a more accurate concentration of limonene in each of the oils **Equation II. 3** was used to calculate the total limonene concentration in each of the oils along with the average peak area of limonene for each of the oils.

Oil	Average Peak Area	% Error	[Limonene] (mM)
Limonene	144674	2.8	7.72
Limonene 1:2 Dilution	59669	6.8	3.86
Limonene 1:4 Dilution	31298	4.7	1.93
Limonene 1:8 Dilution	14596	17	0.965
Limonene 1:16 Dilution	6474	15	0.483
Oil	Average Peak Area	% Error	[Limonene] (mM)	% Limonene
Bergamot	60210	11	3.46	45
Grapefruit	143292	4.6	7.84	101
Lemon	75051	1.6	4.24	55
Lime	65765	0.33	3.75	49
Mandarin	666452	6.2	3.79	49
Neroli	73148	0.56	4.14	54
Orange	120685	2.3	6.65	86
Petitgrain	……	……	……	……
Tangerine	106873	3.5	5.92	77

Table III. 3: Average peak area values for the limonene content in each limonene standard dilution and in each of the oils examined, percent error for each experiment, and total calculated limonene concentration for each sample in mM and percent.

Table III. 3 shows the data collected for the limonene standard curve as well as the data collected for each of the nine oils examined along with the percent error for each experiment and the calculated limonene concentration in each sample in mM and percent.

CHAPTER IV

CONCLUSION

The p-nitrophenol oxidation, the nifedipine oxidation, and the coumarin 7-hydroxylation assays have all become important experiments used to probe the activity of CYP 2E1, CYP 3A4, and CYP 2A6 in the presences of citrus essential oils. Citrus essential oils have been shown in inhibit the activity of CYP 2E1 at concentrations lower than 2.5 µg/mL of inhibitor. Grapefruit oil and orange oil showed to inhibit the activity of CYP 2E1 the greatest of the nine oils examined. None of the oils seemed to inhibit the activity of CYP 3A4 which could be explained by the size of its active site vs. the size of the components in the oils. Citrus essential oils have been shown to inhibit the activity of CYP 2A6 at concentrations as low as 0.5 µg/mL of inhibitor. Bergamot oil and lime oil showed to inhibit the activity of CYP 2A6 the greatest of the nine oils examined.

As predicted the citrus essential oils with the greatest concentration of limonene would inhibit the activity of CYP 2E1 the most. As shown by the amount of limonene present in each of the oils examined grapefruit and orange oils had the highest concentrations of limonene and were the most potent inhibitors of the activity of CYP 2E1. However, the inhibitors ability to inhibit the activities of CYP 2E1 and 2A6 is attributed to not only the limonene content but also another component that is present in the oils. This conclusion is based on the fact that when tested as an inhibitor limonene was not as potent of an inhibitor as grapefruit oil, orange oil, bergamot oil, and lime oil

were on the activities of CYP 2E1 or CYP 2A6. Limonene did not inhibit the activity of CYP 2E1 by >50 % at the highest concentrations of 3.8 µg/mL whereas grapefruit oil and orange oil inhibited the activity of CYP 2E1 by >50 % at concentrations lower than 2.5 µg/mL. Limonene showed moderately good inhibition of CYP 2A6 activity, reaching a >50 % inhibition at a concentration of about 1.3 µg/mL, however, bergamot oil and lime oil both inhibited the activity of CYP 2A6 at concentrations as low as 0.5 µg/mL.

Based on other observations and literature research the inhibition CYP 2E1 and CYP 2A6 activity by grapefruit oil, orange oil, bergamot oil, and lime oil could be due to the presence of limonene as well as the presence of linalol in the oils. Cytochrome P450 inhibition has been shown by citrus essential oils and further research with these oils would lead to a better understanding on their impact on the metabolism, pharmacodynamics, and drug-drug interactions that these citrus essential oils may have.

REFERENCES

1. Lewis, D. F. V., *Journal of Chemical Technology and Biotechnology*. **2002,** 77, 1095-1100.

2. Wu, D.; Cederbaum, A. I., *National Institute of Health: National Institute of Alcohol Abuse and Alcoholism.* **2004.**

3. Reuben, A., *Current Opinion Gastroenterology.* **2008,** 24, 328-338.

4. Satarug, S.; Lang, M. A.; Yongvanit, P.; Sithithaworn, P.; Mairiang, E.; Marirang, P.; Pelkonen, P.; Bartsch, H.; Haswell-Elkins, M. R., *Cancer, Epidemiology, Biomarkers & Prevention.* **1996,** 5, 795-800.

5. Lu, Y.; Cederbaum, A. I., *Free Radical Biology Med.* **2008,** 5, 723-738.

6. Guengerich, F. P.; Martin, M. V.; Beaune, P. H.; Kremers, P.; Wolff, T.; Waxman, D. J., *The Journal of Biological Chemistry.* **1986.** 261, 5051-5060.

7. Xu, C. J.; Li, C. Y. T.; Kong, A. N. T., *Archives of Pharmacal Research.* **2005,** 28, 249-268.

8. Meunier, B.; de Visser, S. P.; Shaik, S., *Chemical Reivews.* **2004,** 104, 3947-3980.

9. Sligar, S. G., *Biochemistry.* **1976,** 15, 5399-5406.

10. Porubsky, P. R.; Meneely, K. M.; Scott, E. E., *Journal of Biological Chemistry.* **2008,** 283, 33698-33707.

11. Park, J. Y.; Harris, D., *Journal of Medicinal Chemistry.* **2003,** 46, 1645-1660.

12. Lewis, D. F. V.; Lake, B. G.; Bird, M. G.; Loizou, G. D.; Dickins, M.; Goldfarb, P. S., *Toxicology in Vitro.* **2003,** 17, 93-105.

13. Ortiz de Montelleno, P. R., Cytochrome P450: Structure, Mechanism, and Biochemistry. **2005,** 3rd ed.

14. Galetin, A.; Clarke, S. E.; Houston, J. B., *Drug Metabolism and Disposition.* **2003,** 31, 1108-1116.

15. Fowler, S. M.; Taylor, J. M.; Friedgerg, T.; Wolf, C. R.; Riley, R. J., *Drug Metabolism and Disposition.* **2002,** 20, 452-456.

16. Fishelovitch, D.; Shaik, S.; Wolfson, H. J.; Nussinov, R., *Journal of Physical Chemistry B.* **2009,** 113, 13018-13025.

17. Lewis, D. F. V.; Lake, B. G.; Dickins, M.; Goldforb, P. S., *Xenobiotica.* **2004,** 34, 549-569.

18. Nowack, R., *Nephrology*, **2008,** 13, 337-347.

19. Sansen, S.; Hsu, M. H.; Stout, C. D.; Johnson, E. F., *Archives of Biochemistry and Biophysics*, **2007,** 464, 197-206.

20. Yano, J. K.; Hsu, M.; Griffin, K. J.; Stout, C. D.; Johnson, E. F., *Nature Structural and Molecular Biology.* **2005,** 12, 822-823.

21. Pelkonen, O.; Rautio, A.; Raunio, H.; Pasanen, M., *Toxicology.* **2000,** 144, 139-147.

22. Bartsch, H.; Nair, U.; Risch, A.; Rojase, M.; Wikman, H.; Alexandrov, K., **2000,** 9, 3-28.

23. He, X. Y.; Shen, J.; Hu, W. Y.; Ding, X. X.; Lu, A. Y. H.; Hong, J. Y., *Archives of Biochemistry and Biophysics*, **2004,** 427, 143-153.

25. Voet, D.; Voet, J.; Pratt, C. W., Fundamentals of Biochemistry: Life at the Molecular Level. **2006,** 2nd ed.

26. Miyazama, M.; Shindo, M.; Shimada, T., *Drug Metabolism and Disposition.* **2002,** 30, 602-607.

27. Girennavar, B.; Jayaprakasha, G. K.; Jadegoud, Y.; Gowda, G. A. N; Patil. B. S., *Bioorganic and Medicinal Chemistry.* **2007,** 15, 3684-3691.

28. Peana, A. T.; D'Aquila, P. S.; Panin, F.; Serra, G.; Pippia, P.; Moretti, M. D. L., *Phytomedicine*, **2002,** 9, 721-726.

29. Seymour, R., *Journal of Clinical Periodontology*, **2003,** 30, 19-21.

30. Shin, S.; Lim, S., *Journal of Applied Microbiology*, **2004,** 97, 1289-1296.

31. Waxman, D. J.; Chang, T. K. H., *Methods in Molecular Biology*, **1998,** 107, 111-116.